ELSEVIER

Computational Geometry 22 (2002) 21–74

Computational Geometry
Theory and Applications

www.elsevier.com/locate/comgeo

# Delaunay refinement algorithms for triangular mesh generation

Jonathan Richard Shewchuk [1]

*Department of Electrical Engineering and Computer Sciences, University of California at Berkeley, Berkeley, CA 94720, USA*

Communicated by S. Fortune; received 11 July 2000; accepted 25 October 2000

**Abstract**

*Delaunay refinement* is a technique for generating unstructured meshes of triangles for use in interpolation, the finite element method, and the finite volume method. In theory and practice, meshes produced by Delaunay refinement satisfy guaranteed bounds on angles, edge lengths, the number of triangles, and the grading of triangles from small to large sizes. This article presents an intuitive framework for analyzing Delaunay refinement algorithms that unifies the pioneering mesh generation algorithms of L. Paul Chew and Jim Ruppert, improves the algorithms in several minor ways, and most importantly, helps to solve the difficult problem of meshing nonmanifold domains with small angles.

Although small angles inherent in the input geometry cannot be removed, one would like to triangulate a domain without creating any *new* small angles. Unfortunately, this problem is not always soluble. A compromise is necessary. A Delaunay refinement algorithm is presented that can create a mesh in which most angles are 30° or greater and no angle is smaller than $\arcsin[(\sqrt{3}/2)\sin(\phi/2)] \sim (\sqrt{3}/4)\phi$, where $\phi \leqslant 60°$ is the smallest angle separating two segments of the input domain. New angles smaller than 30° appear only near input angles smaller than 60°. In practice, the algorithm's performance is better than these bounds suggest.

Another new result is that Ruppert's analysis technique can be used to reanalyze one of Chew's algorithms. Chew proved that his algorithm produces no angle smaller than 30° (barring small input angles), but without any guarantees on grading or number of triangles. He conjectures that his algorithm offers such guarantees. His conjecture is conditionally confirmed here: if the angle bound is relaxed to less than 26.5°, Chew's algorithm produces meshes (of domains without small input angles) that are nicely graded and size-optimal. © 2001 Published by Elsevier Science B.V.

*Keywords:* Triangular mesh generation; Delaunay triangulation; Constrained Delaunay triangulation; Delaunay refinement; Computational geometry

*E-mail address:* jrs@cs.berkeley.edu (J.R. Shewchuk).

[1] Supported in part by the National Science Foundation under Awards ACI-9875170, CMS-9980063, CMS-9318163, and EIA-9802069, in part by the Advanced Research Projects Agency and Rome Laboratory, Air Force Materiel Command, USAF under agreement number F30602-96-1-0287, in part by the Natural Sciences and Engineering Research Council of Canada under a 1967 Science and Engineering Scholarship, and in part by gifts from the Okawa Foundation and Intel.

0925-7721/01/$ – see front matter 
PII: S0925-7721(01)00047-5

## 1. Introduction

*Delaunay refinement* is a technique for generating triangular meshes suitable for use in interpolation, the finite element method, and the finite volume method. The problem is to find a triangulation that covers a specified domain, and contains only triangles whose shapes and sizes satisfy constraints: the angles should not be too small or too large, and the triangles should not be much smaller than necessary, nor larger than desired. Delaunay refinement algorithms offer mathematical guarantees that such constraints can be met. They also perform excellently in practice.

This article has three purposes. First, it offers a theoretical framework for Delaunay refinement algorithms that makes it easy to understand why different variations of Delaunay refinement are successful. This framework is used to clarify the performance of an algorithm by Ruppert, to reanalyze an algorithm by Chew, and to generate several extensions of Delaunay refinement. Second, this article exploits the framework to help find a practical solution to the difficult problem of meshing domains with small angles that Delaunay refinement algorithms proposed to date cannot mesh. Third, it presents almost everything algorithmic a programmer needs to know to implement a state-of-the-art triangular mesh generator for straight-line domains. (Curved boundaries and surfaces, however, are not treated here. Thorough treatments of data structures and Delaunay triangulation algorithms are available elsewhere [8, 17,29].)

A full description of the mesh generation problem begins with the domain to be meshed. Most theoretical treatments of meshing take as their input a *planar straight line graph* (PSLG). A PSLG is a set of vertices and segments, like that illustrated in Fig. 1(a). A segment is an edge that must be represented by a sequence of contiguous edges in the final mesh, as Fig. 1(b) shows. By definition, a PSLG is required to contain both endpoints of every segment it contains, and a segment may intersect vertices and other segments only at its endpoints. (A set of segments that does not satisfy this condition can be converted into a set of segments that does. Run a segment intersection algorithm [3,12,28], then divide each segment into smaller segments at the points where it intersects other segments or vertices.)

The process of mesh generation necessarily divides each segment into smaller edges called *subsegments*. The bold edges in Fig. 1(b) are subsegments; other edges are not. The *triangulation domain* is the region that a user wishes to triangulate. For mesh generation, a PSLG must be *segment-bounded*,

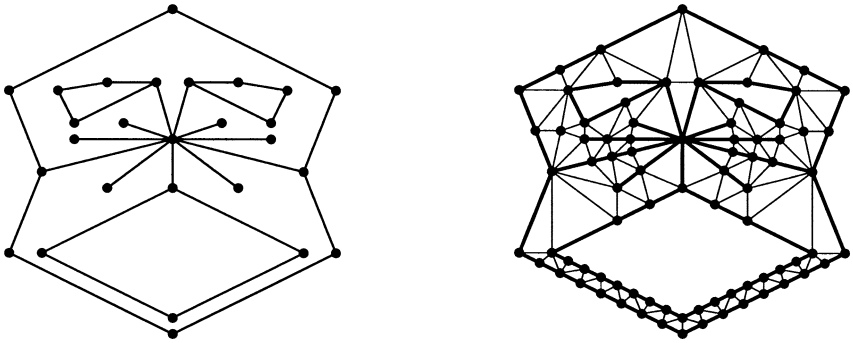

(a) (b)

Fig. 1. A PSLG and a mesh generated by Ruppert's Delaunay refinement algorithm.

meaning that segments of the PSLG entirely cover the boundary separating the triangulation domain from its complement, the *exterior domain.* A triangulation domain need not be convex, and it may enclose untriangulated holes, but the holes must also be bounded by segments. A segment must lie anywhere a triangulated region of the plane meets an untriangulated region.

A mesh generator produces a triangulation that attempts to satisfy three goals. First, the union of the triangles is the triangulation domain, and the triangulation *respects* the segments—each segment is a union of triangulation edges.

Second, the triangles should be relatively "round" in shape, because triangles with large or small angles can degrade the quality of the numerical solution to a finite element problem. In interpolation, triangles with large angles can cause large errors in the gradients of the interpolated surface. In the finite element method, large angles can cause a large *discretization error* [1]; the solution may be less accurate than the method would normally promise. Small angles can cause the coupled systems of algebraic equations that the finite element method yields to be ill-conditioned [7].

A lower bound on the smallest angle of a triangulation implicitly bounds the largest angle. If no angle is smaller than $\theta$, no angle is larger than $180^\circ - 2\theta$. Hence, many mesh generation algorithms, including the Delaunay refinement algorithms studied here, take the approach of attempting to bound the smallest angle.

A third goal is to offer as much control as possible over the sizes of triangles in the mesh. Some meshing algorithms, including algorithms by Baker, Grosse, and Rafferty [2] and Chew [9], produce only *uniform meshes,* in which all triangles have roughly the same size. Other algorithms offer rapid *grading*—the ability to grade from small to large triangles over a relatively short distance. Small, densely packed triangles offer more accuracy than larger, sparsely packed triangles; but the computation time required to solve a problem is proportional to the number of triangles. Hence, choosing a triangle size entails trading off speed and accuracy. In the finite element method, the triangle size required to attain a given amount of accuracy depends upon the behavior of the physical phenomena being modeled, and may vary throughout the problem domain.

Given a *coarse* mesh—one with relatively few triangles—it is not difficult to *refine* it to produce another mesh having a larger number of smaller triangles [18]. The reverse process is not so easy [22]. Hence, mesh generation algorithms often set themselves the goal of being able, in principle, to generate a mesh with as few triangles as possible. They typically offer users the option to refine triangles that are not small enough to yield the required accuracy. The shape of a domain and the requirement for good-quality (round) triangles may necessitate the use of smaller triangles than desired in some portions of the mesh. The three goals are sometimes at odds with each other.

Delaunay refinement algorithms operate by maintaining a Delaunay or constrained Delaunay triangulation, which is refined by inserting carefully placed vertices until the mesh meets constraints on triangle quality and size. This article assumes that the reader is familiar with constrained Delaunay triangulations; consult Lee and Lin [20] and Chew [8] for treatments. Here, the most important property of a Delaunay triangulation is that it has the *empty circumcircle property.* The *circumcircle* of a triangle is the unique triangle that passes through its three vertices. The Delaunay triangulation of a set of vertices is the triangulation (usually, but not always, unique) in which every triangle has an *empty* circumcircle—meaning that the circle encloses no vertex of the triangulation.

A constrained Delaunay triangulation is similar, but respects the input segments as well as the vertices. Two points $p$ and $q$ are *visible* to each other if the open line segment $pq$ (leaving out $p$ and $q$) does not intersect any segment of the input PSLG. The constrained Delaunay triangulation of a PSLG has two

properties. First, no segment intersects the interior of a triangle, because the triangulation must respect the segments. Second, each triangle's circumcircle encloses no vertex that is visible from the interior of the triangle, though it may enclose vertices hidden behind segments.

A few applications, such as some finite volume methods, may have an extra requirement: the mesh must be truly Delaunay (not just constrained Delaunay), and the center of each triangle's circumcircle must lie within the triangulation. This requirement arises because the Voronoi diagram, found by dualizing the Delaunay triangulation, must intersect "nicely" with the triangulation. Only a minority of applications have this requirement, but it is easily met by some of the mesh generation algorithms herein.

Delaunay refinement algorithms are successful because they exploit several favorable characteristics of Delaunay triangulations. One such characteristic is a result by Lawson [19] that a Delaunay triangulation maximizes the minimum angle among all possible triangulations of a point set. This result extends to the constrained Delaunay triangulation, which is optimal among all possible triangulations of a PSLG [20]. Another feature is that inserting a vertex is a local operation, and hence is inexpensive except in unusual cases. The act of inserting a vertex to improve poor-quality triangles in one part of a mesh will not unnecessarily perturb a distant part of the mesh that has no bad triangles. Furthermore, Delaunay triangulations have been extensively studied, and good algorithms for their construction are available [8,15,17,21].

The greatest advantage of Delaunay triangulations is less obvious. The central question of any Delaunay refinement algorithm is, "Where should the next vertex be inserted?". As Section 2 will demonstrate, a reasonable answer is, "As far from other vertices as possible". If a new vertex is inserted too close to another vertex, the resulting small edge will engender thin triangles.

Because a Delaunay triangle has no vertices in its circumcircle, a Delaunay triangulation is an ideal search structure for finding points that are far from other vertices. (It's no coincidence that the circumcenter of each triangle of a Delaunay triangulation is a vertex of the corresponding Voronoi diagram.)

The first provably good Delaunay refinement algorithms were introduced by L. Paul Chew and Jim Ruppert. Ruppert [27] proves that his algorithm produces nicely graded, *size-optimal* meshes with no angle smaller than about 20.7°, if the triangulation domain has no two segments separated by an acute angle. Size optimality means that, for a given bound on the minimum angle, the algorithm produces a mesh whose cardinality (number of triangles) is at most a constant factor larger than the cardinality of the smallest-cardinality mesh that meets the same angle bound. The constant depends upon the angle bound, but is independent of the input PSLG. Alas, the constant is too large to be useful in practice, and the size optimality results are of theoretical interest only. Happily, there are lower bounds on edge lengths whose constants are small enough to be meaningful; these show that the meshes are nicely graded in a formal sense.

Chew [9,10] proves that his algorithms can produce meshes with no angle smaller than 30°, albeit without any guarantees of grading or size optimality. He conjectures that the second of these algorithms offers the same guarantees as Ruppert's algorithm [10].

The foundation of this article is a new framework for analyzing Delaunay refinement—using simple, intuitive flow graphs—that unites Chew's and Ruppert's algorithms and points the way to a variety of improvements. The most important of these is a method that meshes domains with small angles that Chew's and Ruppert's original algorithms cannot mesh.

I describe Ruppert's algorithm, and reprise its analysis using the flow graph framework, in Section 3. In Section 4 I use the framework to conditionally confirm Chew's conjecture: his second published Delaunay refinement algorithm produces nicely graded, size-optimal meshes, if the bound on the smallest allowable angle is relaxed to 26.5°. The difference between this bound and the 20.7° bound of Ruppert's algorithm arises from Chew's method of deciding when to split segments. Examples show that Chew's algorithm behaves better in practice as well. However, the rare applications that require truly Delaunay meshes must still rely upon Ruppert's algorithm.

The algorithms of Ruppert and Chew are largely satisfying in theory and in practice. However, one unresolved problem has limited their applicability: they do not always mesh domains with small angles well—or at all—especially if these domains are nonmanifold (e.g., if there are segments that extend into the interior of the triangulation domain). For example, Ruppert's algorithm sometimes fails to terminate. This problem is not just true of Delaunay refinement algorithms; it stems from a difficulty inherent to triangular mesh generation. Of course, a meshing algorithm must respect the triangulation domain—small input angles cannot be removed. However, one would like to triangulate a domain without creating any small angles that aren't already present in the input. Unfortunately, no algorithm can achieve this goal for all triangulation domains, as Section 5 demonstrates.

Therefore, to be universally applicable, a mesh generation algorithm must make decisions about where to create triangles that have small angles. The most important result of this paper, presented in Section 6, is a new Delaunay refinement algorithm that is guaranteed to terminate and produce a mesh that has poor-quality triangles only in the vicinity of small input angles. Specifically, if the smallest input angle near a triangle is $\phi$, where $\phi \leqslant 60°$, the triangle cannot have an angle smaller than $\arcsin[\sin(\phi/2)/\sqrt{2}]$. Section 6.3 formalizes exactly what "near" means. Ideas related to Chew's algorithm help improve this bound to $\arcsin[(\sqrt{3}/2)\sin(\phi/2)] \sim (\sqrt{3}/4)\phi$ in Section 6.4. A 30° lower bound for all other angles can be established using an idea described in Section 7.3.

Several other extensions of Delaunay refinement are described in Section 7. Pseudocode and details on how to implement the algorithms are presented in Appendix A.

A mesh generator called *Triangle* [29], which implements most of the ideas in this article, is available at http://www.cs.cmu.edu/~quake/triangle.html. Most of the meshes illustrated in this article were generated by Triangle. These examples demonstrate that Delaunay refinement algorithms often strongly outperform their worst-case bounds.

The engineering literature contains many mesh generation algorithms—too many to survey here. Some of these algorithms work well in practice for many applications, but it is likely that nearly all fail on some difficult triangulation domains, because there are no mathematical guarantees. The theoretical literature includes several provably good mesh generation algorithms based on grids or quadtrees, rather than Delaunay refinement. Baker, Grosse, and Rafferty [2] give the first provably good meshing algorithm, which produces triangulations whose angles are bounded between 13° and 90°. The triangles it produces are of uniform size. This shortcoming was addressed by the quadtree-based algorithm of Bern, Eppstein, and Gilbert [5], which is the first size-optimal meshing algorithm. It triangulates polygons so that no angle (except small input angles) is smaller than 18.4°. (This bound cannot be extended to general PSLGs.) Unlike Delaunay refinement algorithms, the Bern et al. algorithm is impractical because it generates far more triangles than are needed in practice; see Section 3 for a visual comparison. For a survey of provably good mesh generation algorithms, see Bern and Eppstein [4].

## 2. The key idea behind Delaunay refinement

In the finite element community, there are a wide variety of measures in use for the quality of a triangle, the most obvious being the smallest and largest angles of the triangle. Miller, Talmor, Teng, and Walkington [23] have pointed out that the most natural and elegant measure for analyzing Delaunay refinement algorithms is the *circumradius-to-shortest edge ratio* of a triangle or tetrahedron. The *circumcenter* and *circumradius* of a triangle are the center and radius of its circumcircle, respectively. The quotient of a triangle's circumradius $r$ and the length $\ell$ of its shortest edge is the metric that is naturally improved by Delaunay refinement algorithms. One would like this ratio to be as small as possible.

Does optimizing this metric aid practical applications? Yes. A triangle's circumradius-to-shortest edge ratio $r/\ell$ is related to its smallest angle $\theta_{\min}$ by the formula $r/\ell = 1/(2\sin\theta_{\min})$. The smaller a triangle's ratio, the larger its smallest angle. If $B$ is an upper bound on the circumradius-to-shortest edge ratio of all triangles in a mesh, then there is no angle smaller than $\arcsin\frac{1}{2B}$ (and vice versa). A triangular mesh generator is wise to make $B$ as small as possible.

The central operation of Chew's and Ruppert's Delaunay refinement algorithms is the insertion of a vertex at the circumcenter of a triangle of poor quality. The Delaunay property is maintained, using Lawson's algorithm [19] or the Bowyer–Watson algorithm [6,32] for the incremental update of Delaunay triangulations. The poor-quality triangle cannot survive, because its circumcircle is no longer empty. For brevity, I refer to the act of inserting a vertex at a triangle's circumcenter as *splitting* a triangle. The idea dates back at least to the engineering literature of the mid-1980s [16]. If poor triangles are split one by one, either all will eventually be eliminated, or the algorithm will run forever.

The main insight behind the Delaunay refinement algorithms (including Chew's, Ruppert's, and the new ones in this article) is that the refinement loop is guaranteed to terminate if the notion of "poor quality" includes only triangles that have a circumradius-to-shortest edge ratio larger than some appropriate bound $B$. The only new edges created by the Delaunay insertion of a vertex $v$ are edges connected to $v$ (see Fig. 2). Because $v$ is the circumcenter of some Delaunay triangle $t$, and there were no vertices inside the circumcircle of $t$ before $v$ was inserted, no new edge can be shorter than the circumradius of $t$. Because $t$ has a circumradius-to-shortest edge ratio larger than $B$, every new edge has length at least $B$ times that of the shortest edge of $t$.

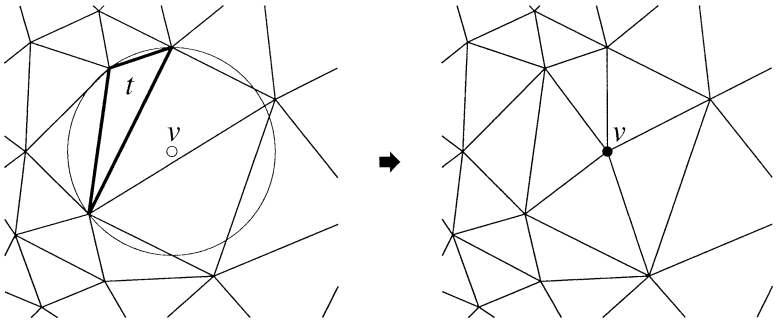


Fig. 2. Any triangle whose circumradius-to-shortest edge ratio is larger than some bound $B$ is split by inserting a vertex at its circumcenter. The Delaunay property is maintained, and the triangle is thus eliminated. Every new edge has length at least $B$ times that of shortest edge of the poor triangle.

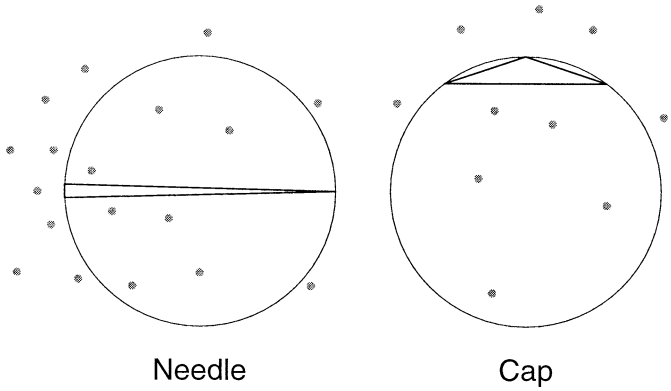


Fig. 3. Skinny triangles have circumcircles larger than their shortest edges. Each skinny triangle may be classified as a needle, whose longest edge is much longer than its shortest edge, or a cap, which has an angle close to 180°. (The classifications are not mutually exclusive.)

Ruppert's algorithm [27] employs a bound of $B = \sqrt{2}$, and Chew's second Delaunay refinement algorithm [10] employs a bound of $B = 1$. Chew's first Delaunay refinement algorithm [9] splits any triangle whose circumradius is greater than the length of the shortest edge in the entire mesh, thus achieving a bound of $B = 1$, but forcing all triangles to have uniform size. With these bounds, every new edge created is at least as long as some other edge already in the mesh. Hence, no vertex is ever inserted closer to another vertex than the length of the shortest edge in the initial triangulation. Delaunay refinement must eventually terminate, because the augmented triangulation will run out of places to put vertices. When it does, all angles are bounded between 20.7° and 138.6° for Ruppert's algorithm, and between 30° and 120° for Chew's.

Henceforth, a triangle whose circumradius-to-shortest edge ratio is greater than $B$ is said to be *skinny*. Fig. 3 provides a different intuition for why all skinny triangles are eventually eliminated by Delaunay refinement. The new vertices that are inserted into a triangulation (grey dots) are spaced roughly according to the length of the shortest nearby edge. Because skinny triangles have relatively large circumradii, their circumcircles are inevitably popped. When enough vertices are introduced that the spacing of vertices is somewhat uniform, large empty circumcircles cannot adjoin small edges, and no skinny triangles can remain in the Delaunay triangulation. Fortunately, the spacing of vertices does not need to be so uniform that the mesh is poorly graded; this fact is formalized in Section 4.3.

These ideas generalize without change to higher dimensions, and are used in several three-dimensional Delaunay refinement algorithms [11,13,30]. Imagine a triangulation that has no boundaries—perhaps it has infinite extent, or perhaps it lies in a periodic space that "wraps around" at the boundaries. Regardless of the dimensionality, Delaunay refinement can eliminate all simplices having a circumradius-to-shortest edge ratio greater than one, without creating any edge shorter than the shortest edge already present.

Unfortunately, my description of Delaunay refinement thus far has a gaping hole: mesh boundaries have not been accounted for. The flaw in the procedure described above is that the circumcenter of a poor triangle might not lie in the mesh at all. Delaunay refinement algorithms, including the algorithms of Chew and Ruppert, are distinguished primarily by how they handle boundaries. Boundaries complicate mesh generation immensely.

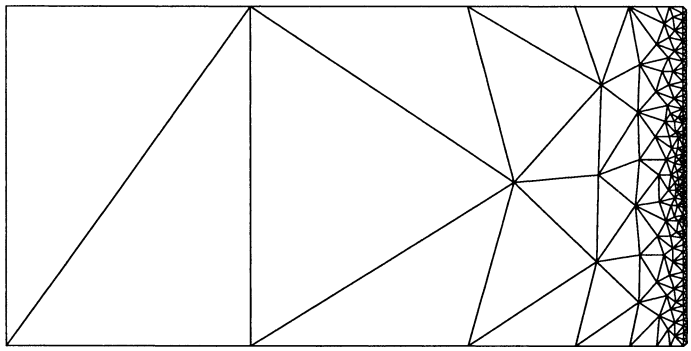

Fig. 4. A demonstration of the ability of Delaunay refinement to achieve large gradations in triangle size while constraining angles. No angle is smaller than 24°.

## 3. Ruppert's Delaunay refinement algorithm

Jim Ruppert's algorithm for two-dimensional quality mesh generation [27] is perhaps the first theoretically guaranteed meshing algorithm to be truly satisfactory in practice. It extends an earlier Delaunay refinement algorithm of Chew [9]. Whereas Chew's first Delaunay refinement algorithm produces uniform meshes, Ruppert's allows the density of triangles to vary quickly over short distances, as illustrated in Fig. 4. The number of triangles produced is typically smaller than the number produced either by Chew's algorithm or the Bern–Eppstein–Gilbert quadtree algorithm [5], as Fig. 5 shows.

Chew independently developed a second Delaunay refinement algorithm quite similar to Ruppert's [10]. I present Ruppert's algorithm first in part because Ruppert's earliest publications of his results [25,26] slightly predate Chew's, and mainly because the algorithm is accompanied by a proof that it produces meshes that are both nicely graded and size-optimal. Sections 4.2 and 4.3 apply Ruppert's analysis method to Chew's second algorithm, which yields better bounds on triangle quality than Ruppert's.

### *3.1. Description of the algorithm*

Ruppert's algorithm is presented here with a few modifications from Ruppert's original presentation. The most significant change is that the algorithm here begins with the constrained Delaunay triangulation of the segment-bounded PSLG provided as input. In contrast, Ruppert's presentation begins with a Delaunay triangulation, and the missing segments are recovered by inserting vertices at the midpoints of the missing segments. Most of the improvements discussed in this article depend on constrained Delaunay triangulations (see Sections 4, 6, and 7.1), so this treatment analyzes the constrained case.

The triangulation must remain constrained Delaunay after each vertex insertion. Fortunately, Lawson's algorithm and the Bowyer–Watson algorithm for incremental vertex insertion can easily be adapted to constrained Delaunay triangulations, simply by never flipping or removing any subsegment. A new vertex cannot cause a triangle to be deleted if a subsegment occludes the visibility between the vertex and the triangle.

Ruppert's algorithm inserts additional vertices until all triangles satisfy the constraints on quality and size set by the user. Some vertices are inserted at triangle circumcenters, and some vertices are inserted

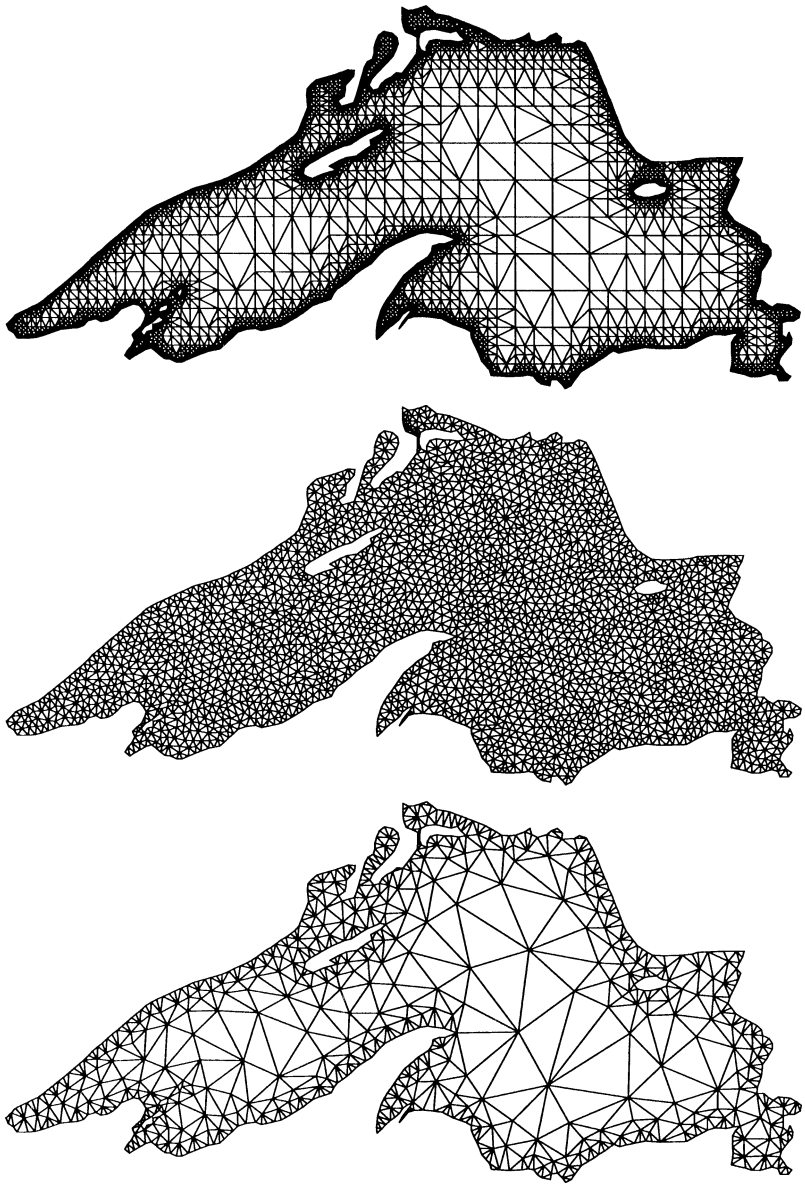

Fig. 5. Meshes generated by the Bern–Eppstein–Gilbert quadtree-based algorithm (top), Chew's first Delaunay refinement algorithm (center), and Ruppert's Delaunay refinement algorithm (bottom). For this polygon, Chew's second Delaunay refinement algorithm produces nearly the same mesh as Ruppert's. (The first mesh was produced by the program `tripoint`, courtesy Scott Mitchell.)

to divide segments into subsegments. The algorithm interleaves segment splitting with triangle splitting. Initially, each segment comprises one subsegment. Vertex insertion is governed by two rules.

- The *diametral circle* of a subsegment is the (unique) smallest circle that encloses the subsegment. A subsegment is said to be *encroached* if a vertex other than its endpoints lies on or inside its

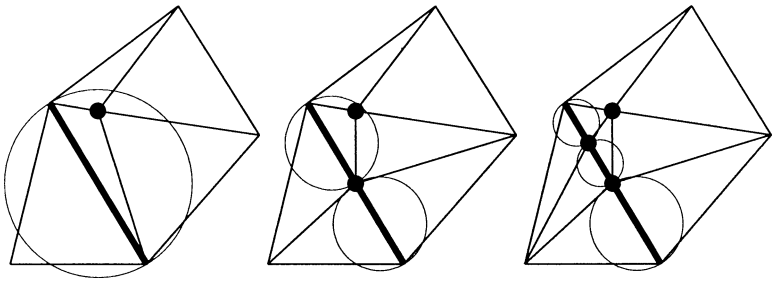

Fig. 6. Segments are split recursively (while maintaining the constrained Delaunay property) until no subsegment is encroached.

diametral circle, and the encroaching vertex is visible from the interior of the subsegment. (Visibility is obstructed only by other segments.) Any encroached subsegment that arises is immediately split into two subsegments by inserting a vertex at its midpoint, as illustrated in Fig. 6. These subsegments have smaller diametral circles, and may or may not be encroached themselves; splitting continues until no subsegment is encroached.

- Each skinny triangle (having a circumradius-to-shortest edge ratio greater than some bound $B$) is normally split by inserting a vertex at its circumcenter, thus eliminating the triangle. However, if the new vertex would encroach upon any subsegment, then it is not inserted; instead, all the subsegments it would encroach upon are split.

Encroached subsegments are given priority over skinny triangles. The order in which subsegments are split, or skinny triangles are split, is arbitrary.

When no encroached subsegments remain, all triangles and edges of the triangulation are Delaunay. A mesh produced by Ruppert's algorithm is Delaunay, and not just constrained Delaunay.

Fig. 7 illustrates the generation of a mesh by Ruppert's algorithm from start to finish. Several characteristics of the algorithm are worth noting. First, if the circumcenter of a skinny triangle is considered for insertion and rejected, it may still be successfully inserted later, after the subsegments it encroaches upon have been split. On the other hand, the act of splitting those subsegments is sometimes enough to eliminate the skinny triangle. Second, the smaller features at the left end of the mesh lead to the insertion of some vertices to the right, but the size of the triangles on the right remains larger than the size of the triangles on the left. The smallest angle in the final mesh is 21.8°.

There is a loose end to tie up. What should happen if the circumcenter of a skinny triangle falls outside the triangulation? Fortunately, the following lemma shows the question is moot.

**Lemma 1.** *Let $T$ be a segment-bounded Delaunay triangulation.* (*Hence, any edge of $T$ that belongs to only one triangle is a subsegment.*) *Suppose that $T$ has no encroached subsegments. Let $v$ be the circumcenter of some triangle $t$ of $T$. Then $v$ lies in $T$.*

**Proof.** Suppose for the sake of contradiction that $v$ lies outside $T$. Let $c$ be the centroid of $t$; $c$ clearly lies inside $T$. Because the triangulation is segment-bounded, the line segment $cv$ must cross some subsegment $s$, as Fig. 8 illustrates. (If there are several such subsegments, let $s$ be the subsegment nearest $c$.) Because $cv$ is entirely enclosed by the circumcircle of $t$, the circumcircle must enclose a

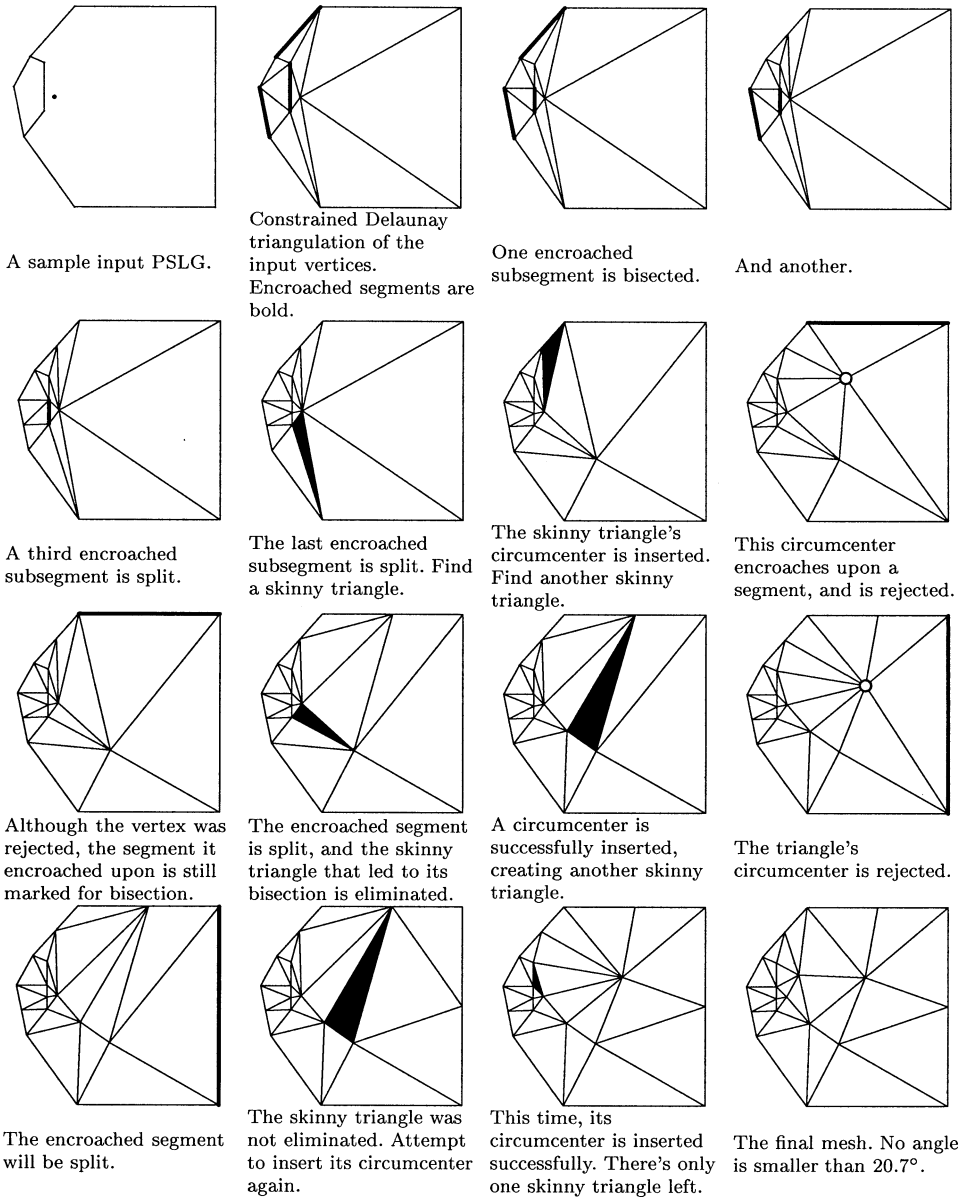


Fig. 7. A complete run of Ruppert's algorithm with an upper bound of $B = \sqrt{2}$ on circumradius-to-shortest edge ratios. The first two images are the input PSLG and the constrained Delaunay triangulation of its vertices. In each image, highlighted subsegments or triangles are about to be split, and open vertices are rejected because they encroach upon a subsegment.

portion of $s$; but the constrained Delaunay property requires that the circumcircle enclose no vertex visible from $c$, so the circumcircle cannot enclose the endpoints of $s$.

Because $c$ and the center of $t$'s circumcircle lie on opposite sides of $s$, the portion of the circumcircle that lies strictly on the same side of $s$ as $c$ (the bold arc in the illustration) is entirely enclosed by the

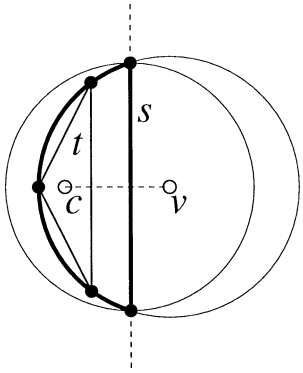


Fig. 8. If the circumcenter $v$ of a triangle $t$ lies outside the triangulation, then some subsegment $s$ is encroached.

diametral circle of $s$. Each vertex of $t$ lies on $t$'s circumcircle and either is an endpoint of $s$, or lies on the same side of $s$ as $c$. Up to two of the vertices of $t$ may be endpoints of $s$, but at least one vertex of $t$ must lie strictly inside the diametral circle of $s$. But $T$ has no encroached subsegments by assumption; the result follows by contradiction. □

Lemma 1 offers the best reason why encroached subsegments are given priority over skinny triangles. Because a circumcenter is inserted only when there are no encroached subsegments, one is assured that the circumcenter will be within the triangulation. The act of splitting encroached subsegments rids the mesh of triangles whose circumcircles lie outside it. The lemma is also reassuring to applications (like some finite volume methods) that require all triangle circumcenters to lie within the triangulation.

In addition to being required to satisfy a quality criterion, triangles can also be required to satisfy a maximum size criterion. In a finite element problem, the triangles must be small enough to ensure that the finite element solution accurately approximates the true solution of some partial differential equation. Ruppert's algorithm can allow the user to specify an upper bound on allowable triangle areas or edge lengths, and the bound may be a function of each triangle's location. Triangles that exceed the local upper bound are split, whether they are skinny or not. So long as the function bounding the sizes of triangles is itself everywhere greater than some positive constant, there is no threat to the algorithm's termination guarantee.

### *3.2. Local feature sizes of planar straight line graphs*

The claim that Ruppert's algorithm produces nicely graded meshes is based on the fact that the spacing of vertices at any location in the mesh is within a constant factor of the sparsest possible spacing. To formalize the idea of "sparsest possible spacing", Ruppert introduces a function called the *local feature size*, which is defined over the plane relative to a specific PSLG.

Given a PSLG $X$, the local feature size $\mathrm{lfs}(p)$ at any point $p$ is the radius of the smallest disk centered at $p$ that intersects two nonincident vertices or segments of $X$. (Two distinct features, each a vertex or segment, are said to be *incident* if they intersect.) Fig. 9 illustrates the notion by giving examples of such disks for a variety of points.

The local feature size of a point is proportional to the sparsest possible spacing of vertices in the neighborhood of that point in any triangulation that respects the segments and has no skinny triangles.

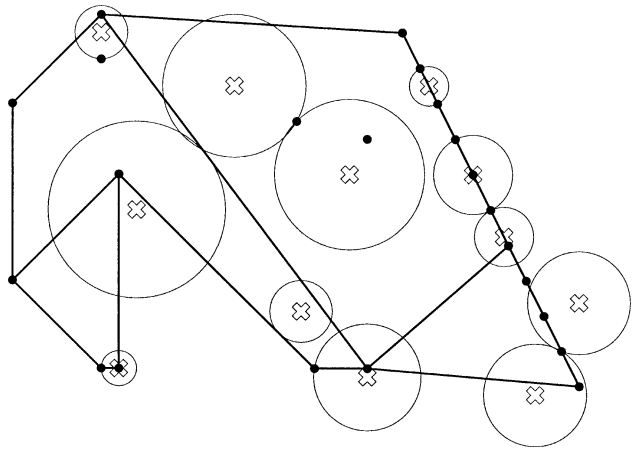

Fig. 9. The radius of each disk illustrated here is the local feature size of the point at its center.

The function $\mathrm{lfs}(\cdot)$ is continuous and has the property that its directional derivatives (where they exist) are bounded in the range $[-1, 1]$. This property leads to a lower bound (within a constant factor to be derived in Section 4.3) on the rate at which edge lengths grade from small to large as one moves away from a small feature. Formally, this is what it means for a mesh to be "nicely graded".

**Lemma 2** (Ruppert [27]). *For any PSLG $X$, and any two points $u$ and $v$ in the plane,*

$$\mathrm{lfs}(v) \leqslant \mathrm{lfs}(u) + |uv|.$$

**Proof.** The disk having radius $\mathrm{lfs}(u)$ centered at $u$ intersects two nonincident features of $X$. The disk having radius $\mathrm{lfs}(u) + |uv|$ centered at $v$ contains the prior disk, and thus also intersects the same two features. Hence, the smallest disk centered at $v$ that intersects two nonincident features of $X$ has radius no larger than $\mathrm{lfs}(u) + |uv|$. □

If the triangulation domain is nonconvex or nonplanar, this lemma can be generalized to use geodesic distances—lengths of shortest paths that are constrained to lie within the triangulation domain—instead of straight-line distances. The proof relies only on the triangle inequality: if $u$ is within a distance of $\mathrm{lfs}(u)$ of each of two nonincident features, then $v$ is within a distance of $\mathrm{lfs}(u) + |uv|$ of each of those same two features. The use of geodesic distances is discussed in detail in Section 7.1.

### *3.3. Proof of termination*

Ruppert's algorithm can eliminate any skinny triangle by inserting a vertex, but new skinny triangles might take its place. How can we be sure the process will ever stop? In this section and in Section 4.3, I present two proofs of the termination of Ruppert's algorithm. The first is included for its intuitive value, and because it offers the best bound on the lengths of the shortest edges. The second proof, adapted from Ruppert, offers better bounds on the lengths of the longer edges of a graded mesh, and thus shows that the algorithm produces meshes that are nicely graded and size-optimal. The presentation here uses a flow graph to expose the intuition behind Ruppert's proof and its natural tendency to bound the circumradius-to-shortest edge ratio.

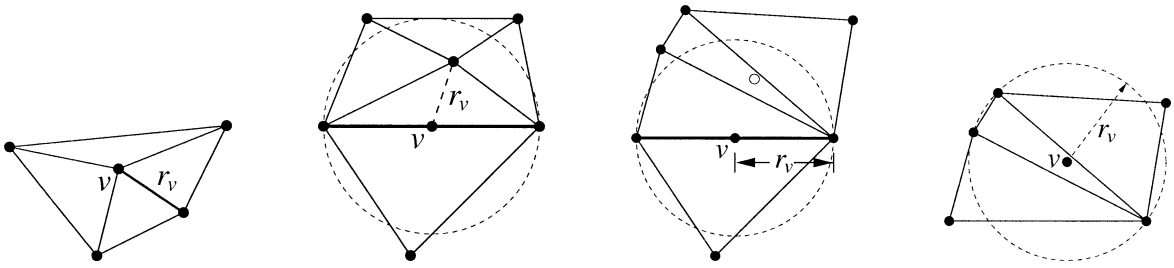


Fig. 10. The insertion radius $r_v$ of a vertex $v$ is the distance to the nearest vertex when $v$ first appears in the mesh. (a) If $v$ is an input vertex, $r_v$ is the distance to the nearest other input vertex. (b) If $v$ is the midpoint of a subsegment encroached upon by a mesh vertex, $r_v$ is the distance to that vertex. (c) If $v$ is the midpoint of a subsegment encroached upon only by a rejected vertex, $r_v$ is the radius of the subsegment's diametral circle. (d) If $v$ is the circumcenter of a skinny triangle, $r_v$ is the radius of the circumcircle.

Both proofs require that $B \geqslant \sqrt{2}$, and that any two incident segments (segments that share an endpoint) in the input PSLG are separated by an angle of 60° or greater. (Ruppert asks for angles of at least 90°, but the weaker bound suffices.) For the second proof, these inequalities must be strict.

A *mesh vertex* is any vertex that has been successfully inserted into the mesh (including the input vertices). A *rejected vertex* is any vertex that is considered for insertion but rejected because it encroaches upon a subsegment. With each mesh vertex or rejected vertex $v$, associate an *insertion radius* $r_v$, equal to the length of the shortest edge connected to $v$ immediately after $v$ is introduced into the triangulation. Consider what this means in three different cases.

- If $v$ is an input vertex, then $r_v$ is the Euclidean distance between $v$ and the nearest input vertex visible from $v$. See Fig. 10(a).
- If $v$ is a vertex inserted at the midpoint of an encroached subsegment, then $r_v$ is the distance between $v$ and the nearest encroaching mesh vertex; see Fig. 10(b). If there is no encroaching mesh vertex (some triangle's circumcenter was considered for insertion but rejected as encroaching), then $r_v$ is the radius of the diametral circle of the encroached subsegment, and hence the length of each of the two subsegments thus produced; see Fig. 10(c).
- If $v$ is a vertex inserted at the circumcenter of a skinny triangle, then $r_v$ is the circumradius of the triangle. See Fig. 10(d).

If a vertex is considered for insertion but rejected because of an encroachment, its insertion radius is defined the same way—as if it had been inserted, even though it is not actually inserted.

Each vertex $v$, including any rejected vertex, has a *parent* vertex $p(v)$, unless $v$ is an input vertex. Intuitively, $p(v)$ is the vertex that is "responsible" for the insertion of $v$. The parent is defined as follows.

- If $v$ is an input vertex, it has no parent.
- If $v$ is a vertex inserted at the midpoint of an encroached subsegment, then $p(v)$ is the encroaching vertex. (Note that $p(v)$ might be a rejected vertex; a parent need not be a mesh vertex.) If there are several encroaching vertices, choose the one nearest $v$.
- If $v$ is a vertex inserted (or rejected) at the circumcenter of a skinny triangle, then $p(v)$ is the most recently inserted endpoint of the shortest edge of that triangle. If both endpoints of the shortest edge are input vertices, choose one arbitrarily.

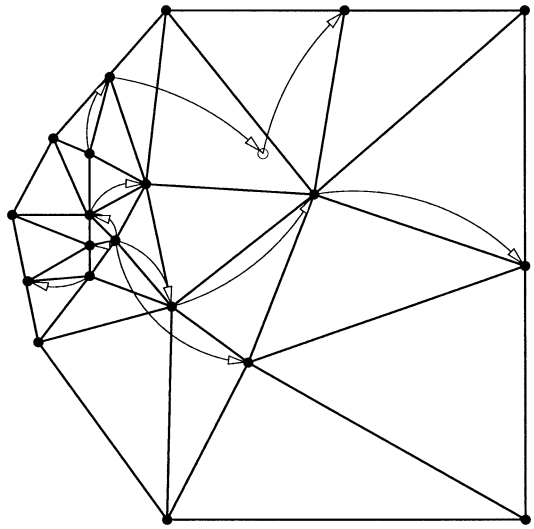

Fig. 11. Trees of vertices for the example of Fig. 7. Arrows are directed from parents to their children. Children include all inserted vertices and one rejected vertex.

Each input vertex is the root of a tree of vertices. However, what is interesting is not each tree as a whole, but the sequence of ancestors of any given vertex, which forms a sort of history of the events leading to the insertion of that vertex. Fig. 11 illustrates the parents of all vertices inserted or considered for insertion during the sample execution of Ruppert's algorithm in Fig. 7.

I will use these definitions to show why Ruppert's algorithm terminates. The key insight is that no descendant of a mesh vertex has an insertion radius smaller than the vertex's own insertion radius—unless the descendant's local feature size is even smaller. Therefore, no edge will ever appear that is shorter than the smallest feature in the input PSLG. To prove these facts, consider the relationship between the insertion radii of a vertex and its parent.

**Lemma 3.** *Let $v$ be a vertex, and let $p = p(v)$ be its parent, if one exists. Then either $r_v \geqslant \mathrm{lfs}(v)$, or $r_v \geqslant C r_p$, where*

- *$C = B$ if $v$ is the circumcenter of a skinny triangle*;
- *$C = 1/\sqrt{2}$ if $v$ is the midpoint of an encroached subsegment and $p$ is the (rejected) circumcenter of a skinny triangle*;
- *$C = 1/(2\cos\alpha)$ if $v$ and $p$ lie on incident segments separated by an angle of $\alpha$ (with $p$ encroaching upon the subsegment whose midpoint is $v$), where $45° \leqslant \alpha < 90°$; and*
- *$C = \sin\alpha$ if $v$ and $p$ lie on incident segments separated by an angle of $\alpha \leqslant 45°$.*

**Proof.** If $v$ is an input vertex, there is another input vertex a distance of $r_v$ from $v$, so $\mathrm{lfs}(v) \leqslant r_v$, and the lemma holds.

If $v$ is inserted at the circumcenter of a skinny triangle, then its parent $p$ is the most recently inserted endpoint of the shortest edge of the triangle; see Fig. 12(a). Hence, the length of the shortest edge of the triangle is at least $r_p$. Because the triangle is skinny, its circumradius-to-shortest edge ratio is at least $B$, so its circumradius is $r_v \geqslant B r_p$.

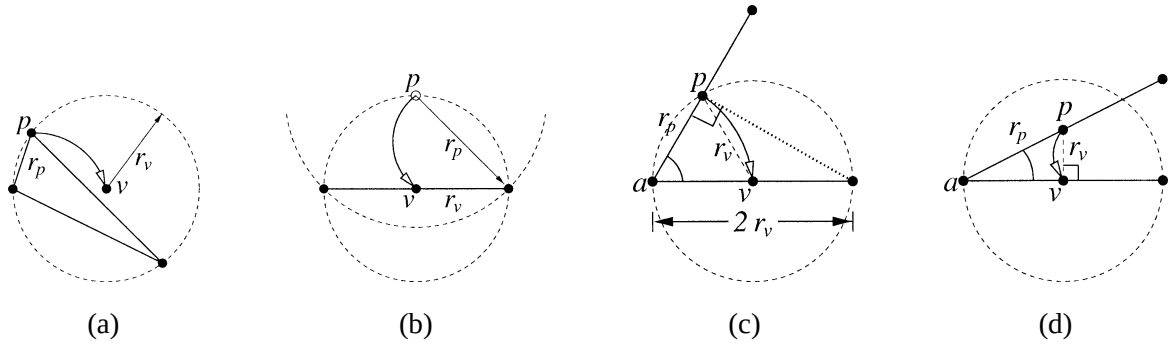


Fig. 12. The relationship between the insertion radii of a child and its parent. (a) When a skinny triangle is split, the child's insertion radius is at least $B$ times larger than that of its parent. (b) When a subsegment is encroached upon by the circumcenter of a skinny triangle, the child's insertion radius may be a factor of $\sqrt{2}$ smaller than the parent's, as this worst-case example shows. (c, d) When a subsegment is encroached upon by a vertex in an incident segment, the relationship depends upon the angle $\alpha$ separating the two segments.

If $v$ is inserted at the midpoint of an encroached subsegment $s$, there are four cases to consider. The first two are all that is needed to prove the termination of Ruppert's algorithm if no angle smaller than $90^\circ$ is present in the input. The last two cases consider the effects of acute angles.

- If the parent $p$ is an input vertex, or was inserted in a segment not incident to the segment containing $s$, then by definition, $\mathrm{lfs}(v) \leqslant r_v$.
- If $p$ is a circumcenter that was considered for insertion but rejected because it encroaches upon $s$, then $p$ lies on or inside the diametral circle of $s$. Because the mesh is constrained Delaunay, one can show that the circumcircle centered at $p$ contains neither endpoint of $s$. Hence, $r_v \geqslant r_p/\sqrt{2}$. See Fig. 12(b) for an example where the relation is equality.
- If $v$ and $p$ lie on incident segments separated by an angle $\alpha$ where $45^\circ \leqslant \alpha < 90^\circ$, the vertex $a$ (for "apex") where the two segments meet obviously cannot lie inside the diametral circle of $s$; see Fig. 12(c). Because $s$ is encroached upon by $p$, $p$ lies on or inside its diametral circle. To find the worst-case (smallest) value of $r_v/r_p$, imagine that $r_p$ and $\alpha$ are fixed; then $r_v = |vp|$ is minimized by making the subsegment $s$ as short as possible, subject to the constraint that $p$ cannot fall outside its diametral circle. The minimum is achieved when $|s| = 2r_v$. Basic trigonometry shows that $|s| \geqslant r_p/\cos\alpha$, and therefore $r_v > r_p/(2\cos\alpha)$.
- If $v$ and $p$ lie on incident segments separated by an angle $\alpha$ where $\alpha \leqslant 45^\circ$, then $r_v/r_p$ is minimized not when $p$ lies on the diametral circle, but when $v$ is the orthogonal projection of $p$ onto $s$, as illustrated in Fig. 12(d). Hence, $r_v \geqslant r_p \sin\alpha$. □

Lemma 3 limits how quickly the insertion radii can decrease through a sequence of descendants of a vertex. If vertices with ever-smaller insertion radii cannot be generated, then edges shorter than existing features cannot be introduced, and Delaunay refinement is guaranteed to terminate.

Fig. 13 expresses this notion as a flow graph. Vertices are divided into three classes: input vertices (which are omitted from the figure because they cannot participate in cycles), *free vertices* inserted at circumcenters of triangles, and *segment vertices* inserted at midpoints of subsegments. Labeled arrows indicate how a vertex can cause the insertion of a child whose insertion radius is some factor times that of its parent. If the graph contains no cycle whose product is less than one, termination is guaranteed.

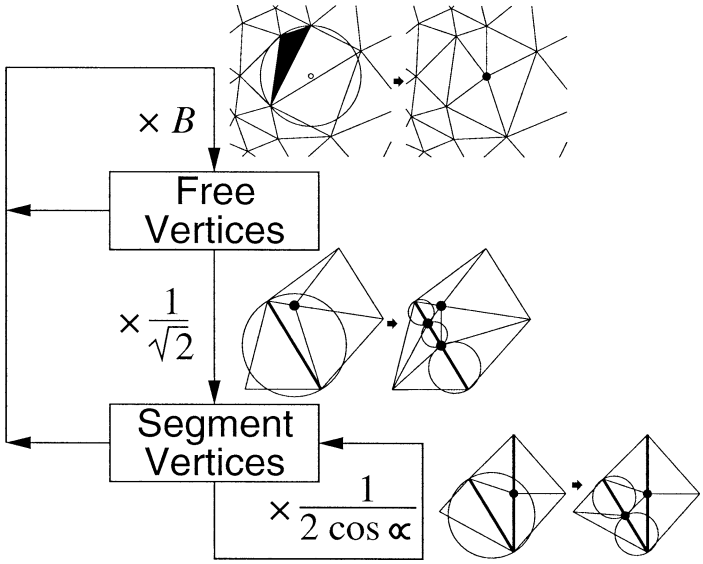


Fig. 13. Flow diagram illustrating the worst-case relation between a vertex's insertion radius and the insertion radii of the children it begets. If no cycles have a product smaller than one, Ruppert's Delaunay refinement algorithm will terminate. Input vertices are omitted from the diagram because they cannot contribute to cycles.

This goal is achieved by choosing $B$ to be at least $\sqrt{2}$, and ensuring that the minimum angle between input segments is at least $60°$. The following theorem formalizes these ideas.

**Theorem 4.** *Let* $\mathrm{lfs}_{\min}$ *be the shortest distance between two nonincident entities* (*vertices or segments*) *of the input PSLG.* [2]

*Suppose that any two incident segments are separated by an angle of at least* $60°$*, and a triangle is considered to be skinny if its circumradius-to-shortest edge ratio is larger than* $B$*, where* $B \geqslant \sqrt{2}$*. Ruppert's algorithm will terminate, with no triangulation edge shorter than* $\mathrm{lfs}_{\min}$.

**Proof.** Suppose for the sake of contradiction that the algorithm introduces an edge shorter than $\mathrm{lfs}_{\min}$ into the mesh. Let $e$ be the first such edge introduced. Clearly, the endpoints of $e$ cannot both be input vertices, nor can they lie on nonincident segments. Let $v$ be the most recently inserted endpoint of $e$.

By assumption, no edge shorter than $\mathrm{lfs}_{\min}$ existed before $v$ was inserted. Hence, for any ancestor $a$ of $v$ that is a mesh vertex, $r_a \geqslant \mathrm{lfs}_{\min}$. Let $p = p(v)$ be the parent of $v$, and let $g = p(p)$ be the grandparent of $v$ (if one exists). Consider the following cases.

- If $v$ is the circumcenter of a skinny triangle, then by Lemma 3, $r_v \geqslant Br_p \geqslant \sqrt{2}r_p$.

[2] Equivalently, $\mathrm{lfs}_{\min} = \min_u \mathrm{lfs}(u)$, where $u$ is chosen from among the input vertices. The proof that both definitions are equivalent is omitted, but it relies on the recognition that if two points lying on nonincident segments are separated by a distance $d$, then at least one of the endpoints of one of the two segments is separated from the other segment by a distance of $d$ or less. Note that $\mathrm{lfs}_{\min}$ is not a lower bound for $\mathrm{lfs}(\cdot)$ over the entire domain; for instance, a segment may have length $\mathrm{lfs}_{\min}$, in which case the local feature size at its midpoint is $\mathrm{lfs}_{\min}/2$.

- If $v$ is the midpoint of an encroached subsegment and $p$ is the circumcenter of a skinny triangle, then by Lemma 3, $r_v \geqslant r_p/\sqrt{2} \geqslant Br_g/\sqrt{2} \geqslant r_g$. (Recall that $p$ is rejected.)
- If $v$ and $p$ lie on incident segments, then by Lemma 3, $r_v \geqslant r_p/(2\cos\alpha)$. Because $\alpha \geqslant 60°$, $r_v \geqslant r_p$.

In all three cases, $r_p \geqslant r_a$ for some ancestor $a$ of $p$ in the mesh. It follows that $r_p \geqslant \text{lfs}_{\min}$, contradicting the assumption that $e$ has length less than $\text{lfs}_{\min}$. It also follows that no edge shorter than $\text{lfs}_{\min}$ is ever introduced, so the algorithm must terminate. □

By design, Ruppert's algorithm terminates only when all triangles in the mesh have a circumradius-to-shortest edge ratio of $B$ or better; hence, at termination, there is no angle smaller than $\arcsin\frac{1}{2B}$. If $B = \sqrt{2}$, the smallest value for which termination is guaranteed, no angle is smaller than 20.7°. Sections 4 and 7 describe several ways to improve this bound.

What about running time? A constrained Delaunay triangulation can be constructed in $O(n \log n)$ time [8], where $n$ is the size of the input PSLG. Once the initial triangulation is complete, well-implemented Delaunay refinement algorithms invariably take time linear in the number of additional vertices that are inserted. See Appendix A for advice on how to achieve this speed. Ruppert (personal communication) exhibits a PSLG on which his algorithm takes $\Theta(h^2)$ time, where $h$ is the size of the final mesh, but the example is contrived and such pathological examples do not arise in practice.

## 4. Chew's second Delaunay refinement algorithm

Paul Chew has published at least two Delaunay refinement algorithms of great interest. The first, not described in this article, produces triangulations of uniform density by dividing segments into subsegments of nearly-uniform length before applying Delaunay refinement [9]. (See Fig. 5, center.) The second, which can produce graded meshes, is discussed here.

Compared to Ruppert's algorithm, Chew's second Delaunay refinement algorithm [10] offers an improved guarantee of good grading in theory, and splits fewer subsegments in practice. This section shows that the algorithm exhibits good grading and size optimality for angle bounds of up to 26.5° (compared with 20.7° for Ruppert's algorithm). Chew shows that his algorithm terminates for an angle bound of up to 30°, albeit with no guarantee of good grading or size optimality. The means by which he obtains this bound is discussed in Section 7.3.

Chew's paper also discusses triangular meshing of curved surfaces in three dimensions, but I consider the algorithm only in its planar context.

### *4.1. Description of the algorithm*

Chew's second Delaunay refinement algorithm begins with the constrained Delaunay triangulation of a segment-bounded PSLG, and eliminates skinny triangles through Delaunay refinement, but Chew does not use diametral circles to determine if subsegments are encroached. Instead, it may arise that a skinny triangle $t$ cannot be split because $t$ and its circumcenter $c$ lie on opposite sides of a subsegment $s$. (Lemma 1 does not apply to Chew's algorithm, so $c$ may even lie outside the triangulation.) Although Chew does not use the word, let us say that $s$ is *encroached* when this circumstance occurs.

Because $s$ is a subsegment, inserting a vertex at $c$ will not remove $t$ from the mesh. Instead, $c$ is rejected, and all free vertices that lie inside the diametral circle of $s$ and are visible from the midpoint of

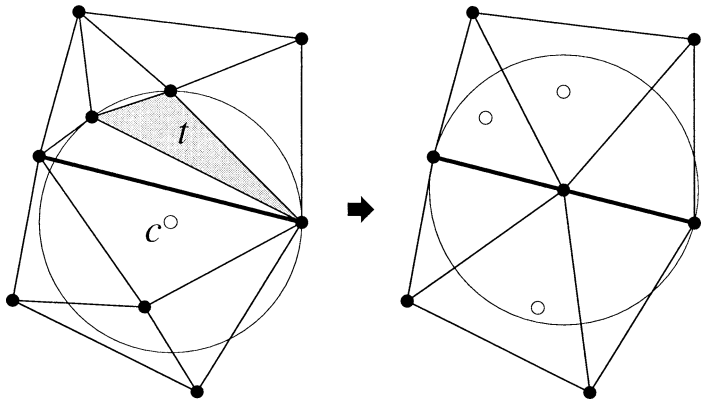


Fig. 14. At left, a skinny triangle and its circumcenter lie on opposite sides of a subsegment. At right, all vertices in the subsegment's diametral circle have been deleted, and a new vertex has been inserted at the subsegment's midpoint.

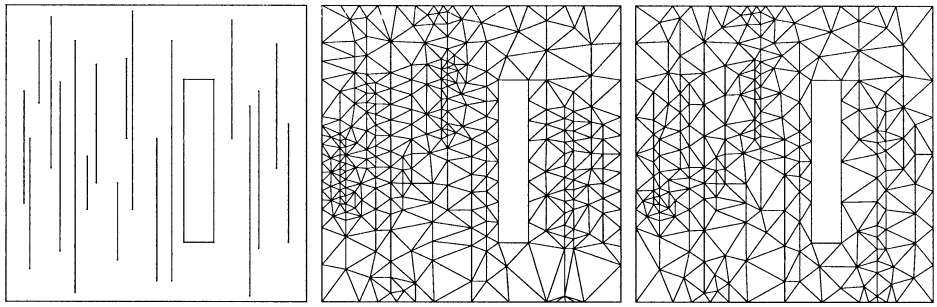

Fig. 15. A PSLG, a 559-triangle mesh produced by Ruppert's algorithm, and a 423-triangle mesh produced by Chew's second algorithm. No angle in either mesh is smaller than 25°.

*s* are deleted from the triangulation. (Input vertices and segment vertices are not deleted.) Then, a new vertex is inserted at the midpoint of *s*. The constrained Delaunay property is maintained throughout all vertex deletions and insertions. Fig. 14 illustrates a subsegment split in Chew's algorithm.

If several subsegments lie between *t* and *c*, only the subsegment nearest *t* is split. If no subsegment lies between *t* and *c*, but *c* lies precisely on a subsegment, then that subsegment is considered encroached and split at its midpoint.

Chew's second algorithm produces a mesh that is not guaranteed to be Delaunay (only constrained Delaunay). For the few applications that require truly Delaunay triangles, Ruppert's algorithm is preferable. For the majority of applications, however, Chew has two advantages. First, some subsegment splits are avoided that would otherwise have occurred, so the final mesh may have fewer triangles, depending on the edge lengths of the PSLG. Consider two contrasting examples. In Fig. 5 (bottom), the segments are so short that few are ever encroached, so Ruppert and Chew generate virtually the same mesh. In Fig. 15, the segments are long compared to their local feature sizes, and Chew produces many fewer triangles.

The second advantage is that when a subsegment is split by a vertex $v$ with parent $p$, a better bound can be found for the ratio between $r_v$ and $r_p$ than Lemma 3's bound. This improvement leads to better bounds on the minimum angle, edge lengths, and mesh cardinality.

### *4.2. Proof of termination*

If no input angle is less than 60°, Chew's algorithm terminates for any bound on circumradius-to-shortest edge ratio $B$ such that $B \geqslant \sqrt{5}/2 \doteq 1.12$. Therefore, the smallest angle can be bounded by up to $\arcsin(1/\sqrt{5}) \doteq 26.56°$. Section 7.3 discusses how Chew improves this bound to 30°, but the weaker result is discussed here because it is the first step to proving (in Section 4.3) that Chew's algorithm offers guaranteed good grading and size optimality for angle bounds less than 26.56°. PSLGs with angles less than 60° are treated in Section 6.4.

By the reasoning of Lemma 1, if a triangle and its circumcenter lie on opposite sides of a subsegment, or if the circumcenter lies on the subsegment, then some vertex of the triangle (other than the subsegment's endpoints) lies on or inside the subsegment's diametral circle. Hence, Chew's algorithm never splits a subsegment that Ruppert's algorithm would not split. It follows that the inequalities in Lemma 3 are as true for Chew's algorithm as they are for Ruppert's algorithm. However, Chew will often decline to split a subsegment that Ruppert would split, and thus splits fewer subsegments overall. A consequence is that the relationship between the insertion radii of a subsegment midpoint and its parent can be tightened.

**Lemma 5.** *Let $\theta = \arcsin \frac{1}{2B}$ be the angle bound below which a triangle is considered skinny. Let $s$ be a subsegment that is encroached because some skinny triangle $t$ and its circumcenter $c$ lie on opposite sides of $s$ (or $c$ lies on $s$). Let $v$ be the vertex inserted at the midpoint of $s$. Then one of the following four statements is true.* (*Only the fourth differs from Lemma 3.*)

- $r_v \geqslant \mathrm{lfs}(v)$;
- $r_v \geqslant r_p/(2\cos\alpha)$, *where $p$ is a vertex that encroaches upon $s$ and lies in a segment separated by an angle of $\alpha \geqslant 45°$ from the segment containing $s$*;
- $r_v \geqslant r_p \sin\alpha$, *where $p$ is as above, with $\alpha \leqslant 45°$; or*
- *there is some vertex $p$* (*which is deleted from inside the diametral circle of $s$ or lies precisely on the diametral circle*) *such that $r_v \geqslant r_p \cos\theta$.*

**Proof.** Chew's algorithm deletes all free vertices inside the diametral circle of $s$ that are visible from $v$. If any vertex remains visible from $v$ inside the diametral circle, it is an input vertex or a segment vertex. Define the parent $p$ of $v$ to be the closest such vertex. If $p$ is an input vertex or lies on a segment not incident to the segment that contains $s$, then $\mathrm{lfs}(v) \leqslant r_v$ and the lemma holds. If $p$ lies on an incident segment, then $r_v \geqslant r_p/(2\cos\alpha)$ for $\alpha \geqslant 45°$ or $r_v \geqslant r_p \cos\theta$ for $\alpha \leqslant 45°$ as in Lemma 3.

Otherwise, no vertex inside the diametral circle of $s$ is visible after the deletions, so $r_v$ is equal to the radius of the diametral circle. This is the reason why Chew's algorithm deletes the vertices: when $v$ is inserted, the nearest visible vertices are the subsegment endpoints, and no short edge appears.

Mentally jump back in time to just before the vertex deletions. Assume without loss of generality that $t$ lies above $s$, with $c$ below. Following Lemma 1, at least one vertex of $t$ lies on or inside the upper half of the diametral circle of $s$. There are two cases, depending on the total number of vertices on or inside this semicircle.

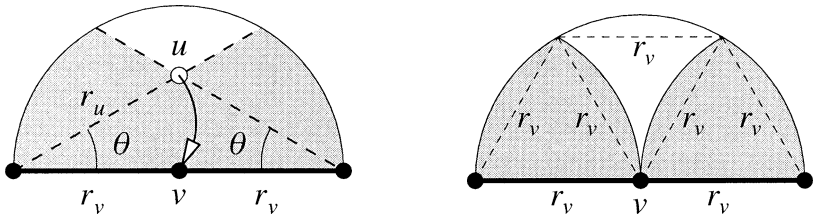


Fig. 16. (a) The case where exactly one vertex is in the semicircle. (b) The case where more than one vertex is in the semicircle.

If the upper semicircle encloses only one vertex $u$ visible from $v$, then $t$ is the triangle whose vertices are $u$ and the endpoints of $s$. Because $t$ is skinny, $u$ must lie in the shaded region of Fig. 16(a). The insertion radius $r_u$ cannot be greater than the distance from $u$ to the nearest endpoint of $s$, so $r_v \geqslant r_u \cos\theta$. (For a fixed $r_v$, $r_u$ is maximized when $u$ lies at the apex of the isosceles triangle whose base is $s$ and whose base angles are $\theta$.) Define the parent of $v$ to be $u$.

If the upper semicircle encloses more than one vertex visible from $v$, consider Fig. 16(b), in which the shaded region represents points within a distance of $r_v$ from an endpoint of $s$. If some vertex $u$ lies in the shaded region, then $r_u \leqslant r_v$; define the parent of $v$ to be $u$. If no vertex lies in the shaded region, then there are at least two vertices visible from $v$ in the white region of the upper semicircle. Let $u$ be the most recently inserted of these vertices. The vertex $u$ is at a distance of at most $r_v$ from any other vertex in the white region, so $r_u \leqslant r_v$; define the parent of $v$ to be $u$. □

Lemma 5 extends the definition of parent to accommodate the new type of encroachment defined in Chew's algorithm. When a subsegment $s$ is encroached, the parent $p$ of its newly inserted midpoint $v$ is defined to be a vertex on or inside the diametral circle of $s$, just as in Ruppert's algorithm.

Chew's algorithm can be shown to terminate in the same manner as Ruppert's. Do the differences between Chew's and Ruppert's algorithms invalidate any of the assumptions used in Theorem 4 to prove termination? The most important difference is that vertices may be deleted from the mesh. When a vertex is deleted from a constrained Delaunay triangulation, no surviving vertex finds itself adjoining a shorter edge than the shortest edge it adjoined before the deletion. (This fact follows because a constrained Delaunay triangulation connects every vertex to its nearest visible neighbor.) Hence, each vertex's insertion radius still serves as a lower bound on the lengths of all edges that connect the vertex to vertices older than itself.

If vertices can be deleted, are we certain that the algorithm will run out of places to put new vertices? Observe that vertex deletions only occur when a subsegment is split, and vertices are never deleted from segments. Theorem 4 sets a lower bound on the length of each subsegment, so only a finite number of subsegment splits can occur. After the last subsegment split, no more vertex deletions occur, and eventually there will be no space left for new vertices. Therefore, Theorem 4 holds for Chew's algorithm as well as Ruppert's.

The consequence of the bound proven by Lemma 5 is illustrated in the flow graph of Fig. 17. Recall that termination is guaranteed if no cycle has a product less than one. Hence, a condition of termination is that $B\cos\theta \geqslant 1$. As $\theta = \arcsin\frac{1}{2B}$, the best bound that satisfies this criterion is $B = \sqrt{5}/2 \doteq 1.12$, which corresponds to an angle bound of $\arcsin(1/\sqrt{5}) \doteq 26.56°$.

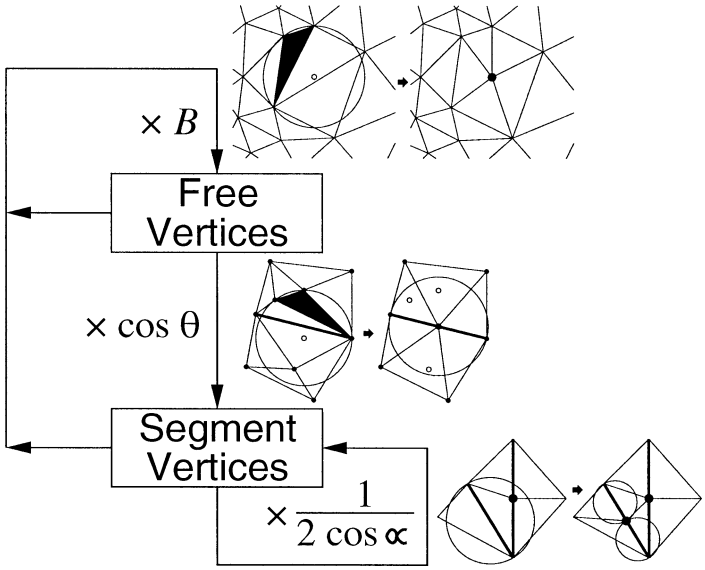


Fig. 17. Flow diagram for Chew's algorithm.

### 4.3. Good grading and size optimality in Ruppert's and Chew's algorithms

Theorem 4 guarantees that no edge of a mesh produced by Ruppert's algorithm is shorter than $\text{lfs}_{\min}$, and the proof extends to Chew's algorithm. This guarantee may be satisfying for a user who desires a uniform mesh, but it is not satisfying for a user who requires a spatially graded mesh. What follows is a proof that each edge of the output mesh has length proportional to the local feature sizes of its endpoints. Hence, edge lengths are determined by local considerations; features lying outside the disk that defines the local feature size of a point can only weakly influence the lengths of edges that contain that point. Triangle sizes vary quickly over short distances where such variation is desirable to help reduce the number of triangles in the mesh.

The main point of this section is to demonstrate that Chew's algorithm offers better theoretical guarantees about triangle quality, edge lengths, and good grading than Ruppert's. (We should not forget, though, that it is Ruppert's analysis technique that allows us to draw this conclusion.) Whereas Ruppert only guarantees good grading and size optimality for angle bounds less than about 20.7°, Chew can make these promises for angle bounds less than about 26.5°, and offer better bounds on edge lengths for the angle bounds where Ruppert's guarantees do hold. However, the differences are not as pronounced in practice as in theory, and readers whose interests are purely practical may skip this section without affecting their understanding of the rest of the article.

Lemmata 3 and 5 were concerned with the relationship between the insertion radii of a child and its parent. The next lemma is concerned with the relationship between $\text{lfs}(v)/r_v$ and $\text{lfs}(p)/r_p$. For any vertex $v$, define $D_v = \text{lfs}(v)/r_v$. Think of $D_v$ as the one-dimensional density of vertices near $v$ when $v$ is inserted, weighted by the local feature size. One would like this density to be as small as possible. $D_v \leqslant 1$ for any input vertex, but $D_v$ tends to be larger for a vertex inserted late.

**Lemma 6.** *Let $v$ be a vertex with parent $p = p(v)$. Suppose that $r_v \geqslant C r_p$ (following Lemmata 3 and 5). Then $D_v \leqslant 1 + D_p/C$.*

**Proof.** By Lemma 2, $\mathrm{lfs}(v) \leqslant \mathrm{lfs}(p) + |vp|$. By definition, the insertion radius $r_v$ is $|vp|$ if $p$ is a mesh vertex, whereas if $p$ is a rejected circumcenter, then $r_v \geqslant |vp|$. Hence, we have

$$\mathrm{lfs}(v) \leqslant \mathrm{lfs}(p) + r_v = D_p r_p + r_v \leqslant \frac{D_p}{C} r_v + r_v.$$

The result follows by dividing these expressions by $r_v$. □

Let's consider Ruppert's algorithm first, and then compare Chew's.

**Lemma 7** (Ruppert [27]). *Consider a mesh produced by Ruppert's algorithm. Suppose the quality bound $B$ is strictly larger than $\sqrt{2}$, and the smallest angle between two incident segments in the input PSLG is strictly greater than $60°$. There exist fixed constants $D_T \geqslant 1$ and $D_S \geqslant 1$ such that, for any vertex $v$ inserted (or considered for insertion and rejected) at the circumcenter of a skinny triangle, $D_v \leqslant D_T$, and for any vertex $v$ inserted at the midpoint of an encroached subsegment, $D_v \leqslant D_S$. Hence, the insertion radius of every vertex has a lower bound proportional to its local feature size.*

**Proof.** Consider any non-input vertex $v$ with parent $p = p(v)$. If $p$ is an input vertex, then $D_p = \mathrm{lfs}(p)/r_p \leqslant 1$. Otherwise, assume for the sake of induction that the lemma is true for $p$, so that $D_p \leqslant D_T$ if $p$ is a circumcenter, and $D_p \leqslant D_S$ if $p$ is a midpoint. Hence, $D_p \leqslant \max\{D_T, D_S\}$.

First, suppose $v$ is inserted or considered for insertion at the circumcenter of a skinny triangle. By Lemma 3, $r_v \geqslant B r_p$. Thus, by Lemma 6, $D_v \leqslant 1 + \max\{D_T, D_S\}/B$. It follows that one can prove that $D_v \leqslant D_T$ if $D_T$ is chosen so that

$$1 + \frac{\max\{D_T, D_S\}}{B} \leqslant D_T. \tag{1}$$

Second, suppose $v$ is inserted at the midpoint of a subsegment $s$. If its parent $p$ is an input vertex or lies on a segment not incident to $s$, then $\mathrm{lfs}(v) \leqslant r_v$, and the theorem holds. If $p$ is the circumcenter of a skinny triangle (considered for insertion but rejected because it encroaches upon $s$), $r_v \geqslant r_p/\sqrt{2}$ by Lemma 3, so by Lemma 6, $D_v \leqslant 1 + \sqrt{2} D_T$.

Alternatively, if $p$, like $v$, is a segment vertex, and $p$ and $v$ lie on incident segments, then $r_v \geqslant r_p/(2\cos\alpha)$ by Lemma 3, and thus by Lemma 6, $D_v \leqslant 1 + 2D_S \cos\alpha$. It follows that one can prove that $D_v \leqslant D_S$ if $D_S$ is chosen so that

$$1 + \sqrt{2} D_T \leqslant D_S, \quad \text{and} \tag{2}$$

$$1 + 2D_S \cos\alpha \leqslant D_S. \tag{3}$$

If the quality bound $B$ is strictly larger than $\sqrt{2}$, inequalities (1) and (2) are simultaneously satisfied by choosing

$$D_T = \frac{B+1}{B-\sqrt{2}}, \qquad D_S = \frac{(1-\sqrt{2})B}{B-\sqrt{2}}.$$

If the smallest input angle $\alpha_{\min}$ is strictly greater than $60°$, inequalities (3) and (1) are satisfied by choosing

$$D_S = \frac{1}{1 - 2\cos\alpha_{\min}}, \qquad D_T = 1 + \frac{D_S}{B}.$$

One of these choices will dominate, depending on the values of $B$ and $\alpha_{\min}$. In either case, if $B > \sqrt{2}$ and $\alpha_{\min} > 60°$, there are values of $D_T$ and $D_S$ that satisfy all the inequalities. □

Note that as $B$ approaches $\sqrt{2}$ or $\alpha$ approaches 60°, $D_T$ and $D_S$ approach infinity. In practice, the algorithm is better behaved than the theoretical bound suggests; the vertex density approaches infinity only after $B$ drops below one.

**Theorem 8** (Ruppert [27]). *For any vertex $v$ of the output mesh, the distance to its nearest neighbor $w$ is at least* $\mathrm{lfs}(v)/(D_S + 1)$.

**Proof.** Inequality (2) indicates that $D_S > D_T$, so Lemma 7 shows that $\mathrm{lfs}(v)/r_v \leqslant D_S$ for any vertex $v$. If $v$ was added after $w$, then the distance between the two vertices is $r_v \geqslant \mathrm{lfs}(v)/D_S$, and the theorem holds. If $w$ was added after $v$, apply the lemma to $w$, yielding

$$|vw| \geqslant r_w \geqslant \frac{\mathrm{lfs}(w)}{D_S}.$$

By Lemma 2, $\mathrm{lfs}(w) + |vw| \geqslant \mathrm{lfs}(v)$, so

$$|vw| \geqslant \frac{\mathrm{lfs}(v) - |vw|}{D_S}.$$

It follows that $|vw| \geqslant \mathrm{lfs}(v)/(D_S + 1)$. □

To give a specific example, consider triangulating a PSLG (having no acute input angles) so that no angle of the output mesh is smaller than 15°; hence $B \doteq 1.93$. For this choice of $B$, $D_T \doteq 5.66$ and $D_S \doteq 9.01$. Hence, the spacing of vertices is at worst about ten times smaller than the local feature size. Away from boundaries, the spacing of vertices is at worst seven times smaller than the local feature size.

Fig. 18 illustrates the algorithm's grading for a variety of angle bounds. Ruppert's algorithm typically terminates for angle bounds much higher than the theoretically guaranteed 20.7°, and typically exhibits much better vertex spacing than the provable worst-case bounds imply.

Let's compare Chew's algorithm.

**Lemma 9.** *Consider a mesh produced by Chew's algorithm. Suppose the quality bound $B$ is strictly larger than $\sqrt{5}/2$, and the smallest angle between two incident segments in the input PSLG is strictly greater than* 60°. *There exist fixed constants $D_T \geqslant 1$ and $D_S \geqslant 1$ such that, for any vertex $v$ inserted at the circumcenter of a skinny triangle, $D_v \leqslant D_T$, and for any vertex $v$ inserted at the midpoint of an encroached subsegment, $D_v \leqslant D_S$.*

**Proof.** Essentially the same as the proof of Lemma 7, except that Lemma 5 makes it possible to replace inequality (2) with

$$D_S \geqslant 1 + \frac{D_T}{\cos\theta} \geqslant 1 + \frac{2BD_T}{\sqrt{4B^2 - 1}}. \tag{4}$$

If the quality bound $B$ is strictly larger than $\sqrt{5}/2$, inequalities (1) and (4) are simultaneously satisfied by choosing

$$D_T = \frac{(1 + \frac{1}{B})\sqrt{4B^2 - 1}}{\sqrt{4B^2 - 1} - 2}, \qquad D_S = \frac{\sqrt{4B^2 - 1} + 2B}{\sqrt{4B^2 - 1} - 2}.$$

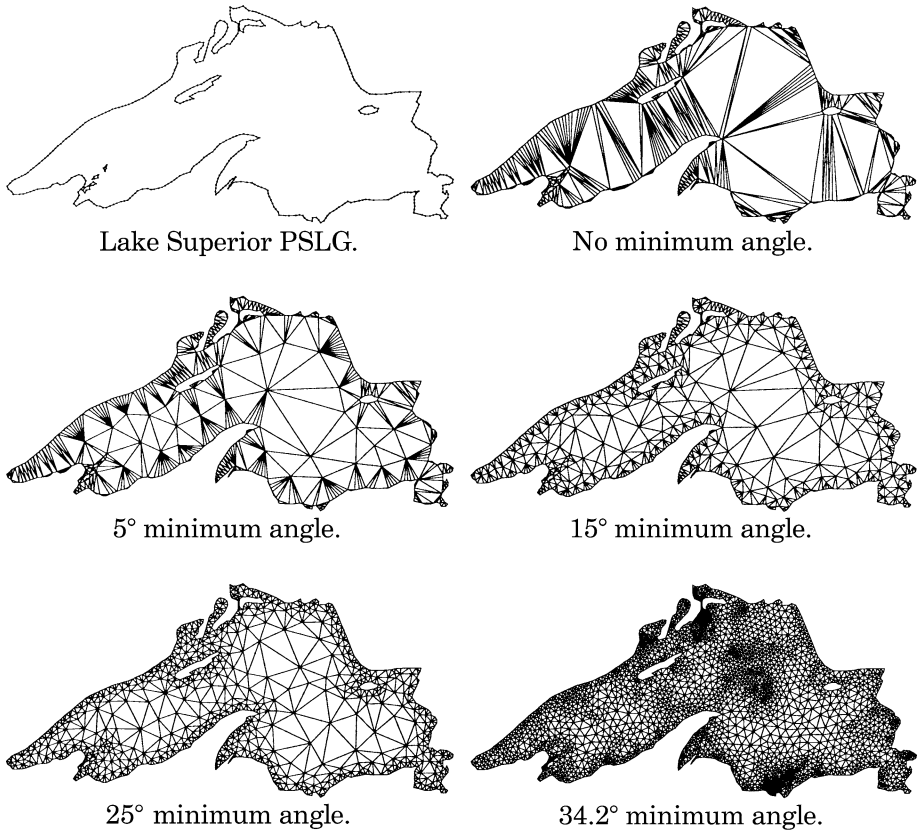


Fig. 18. Meshes generated with Ruppert's algorithm for several different angle bounds. The algorithm does not terminate for angle bounds of 34.3° or higher on this PSLG.

$D_T$ and $D_S$ must also satisfy inequality (3), so larger values of $D_T$ and $D_S$ may be needed, as in Lemma 7. However, if $B > \sqrt{5}/2$ and $\alpha_{\min} > 60°$, there are values of $D_T$ and $D_S$ that satisfy all the inequalities.

Theorem 8 applies to Chew's algorithm as well as Ruppert's, but the values of $D_T$ and $D_S$ are different. Again consider triangulating a PSLG (free of acute angles) so that no angle of the output mesh is smaller than 15°. Then $D_T \doteq 3.27$, and $D_S \doteq 4.39$, compared to the corresponding values of 5.66 and 9.01 for Ruppert's algorithm. Hence, the spacing of vertices is at worst a little more than five times the local feature size, and a little more than four times the local feature size away from segments.

Ruppert [27] uses Theorem 8 to prove the size optimality of the meshes his algorithm generates, and his result has been improved by Mitchell [24]. Mitchell's theorem is stated below, but the lengthy proof is omitted.

**Theorem 10** (Mitchell [24]). *Let* $\mathrm{lfs}_T(p)$ *be the local feature size at* $p$ *with respect to a triangulation* $T$ (*treating* $T$ *as a PSLG*), *whereas* $\mathrm{lfs}(p)$ *remains the local feature size at* $p$ *with respect to the input PSLG. Suppose a triangulation* $T$ *with smallest angle* $\theta$ *has the property that there is some constant* $k_1 \geqslant 1$ *such that for every point* $p$, $k_1 \mathrm{lfs}_T(p) \geqslant \mathrm{lfs}(p)$. *Then the cardinality* (*number of triangles*) *of* $T$

*is less than $k_2$ times the cardinality of any other triangulation of the input PSLG with smallest angle $\theta$, where $k_2 \in O(k_1^2/\theta)$.*

Theorem 8 can be used to show that the precondition of Theorem 10 is satisfied by meshes generated by Ruppert's and Chew's algorithms (with $k_1 \propto D_S$). Hence, the cardinality of a mesh generated by either algorithm is within a constant factor of the cardinality of the best possible mesh satisfying the angle bound. However, the constant factor hidden in Mitchell's theorem is much too large to be a meaningful guarantee in practice.

Because the worst-case number of triangles is proportional to the square of $D_S$, Chew's algorithm is size-optimal with a constant of optimality almost four times better than Ruppert's algorithm. However, worst-case behavior is never seen in practice, and the observed difference between the two algorithms is less dramatic.

## 5. A negative result on quality triangulations of PSLGs that have small angles

For any angle bound $\theta > 0$, there exists a PSLG $X$ such that it is not possible to triangulate $X$ without creating a new corner (not present in $X$) whose angle is smaller than $\theta$. This statement imposes a fundamental limitation on any triangular mesh generation algorithm.

The result holds for certain PSLGs that have an angle much smaller than $\theta$. Of course, one must respect the PSLG; small input angles cannot be removed. However, one would like to believe that it is possible to triangulate a PSLG without creating any small angles that aren't already present in the input. Unfortunately, no algorithm can make this guarantee for all PSLGs.

The reasoning behind the claim is as follows. Suppose two collinear subsegments of lengths $a$ and $b$ share a common endpoint, as illustrated in Fig. 19. Mitchell [24] proves that if the triangles incident on the common endpoint have no angle smaller than $\theta$, then the ratio $b/a$ has an upper bound of $(2\cos\theta)^{180°/\theta}$. (This bound is tight if $180°/\theta$ is an integer. Fig. 19 offers an example where the bound is obtained.) Hence, any bound on the smallest angle of a triangulation imposes a limit on the grading of triangle sizes.

A problem can arise if three segments intersect at a vertex $o$, with two segments separated by a tiny angle $\phi$ and two separated by a much larger angle. Fig. 20 (top) illustrates this circumstance. Suppose that the middle segment of the three has been split into two segments by a vertex in the middle.

Assume for the sake of contradiction that there is a triangulation $T$ that respects this domain and has no angle smaller than $\theta$, except for the one small input angle at $o$. Let $p$ be the vertex of $T$ that lies on the middle segment closest to $o$, so that $po$ is an edge of $T$. The placement of $p$ forces the narrow wedge

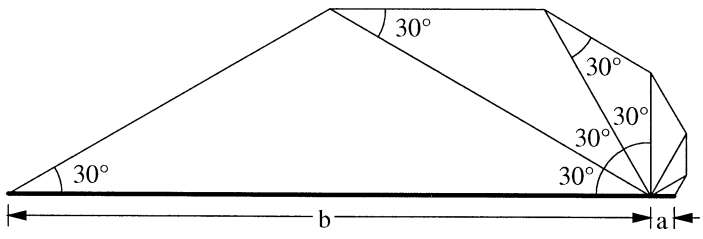


Fig. 19. In any triangulation with no angle smaller than 30°, the ratio $b/a$ cannot exceed 27.

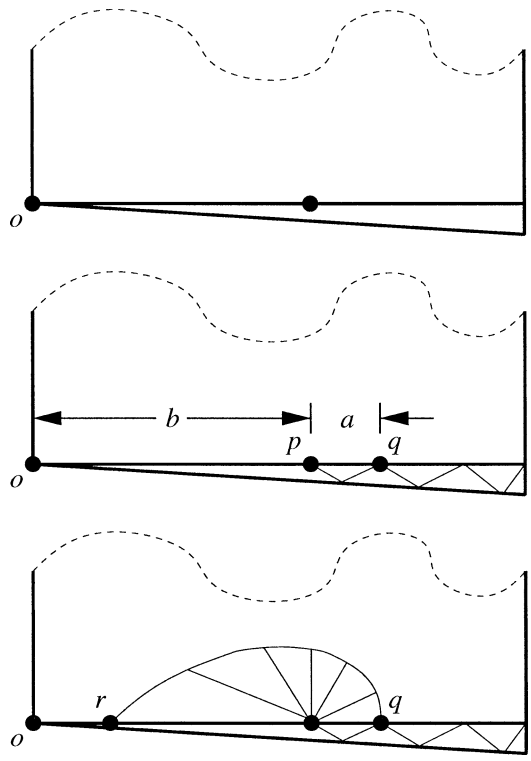


Fig. 20. Top: a difficult PSLG with a small interior angle $\phi$. Center: the vertex $p$ and the angle constraint necessitate the placement of the vertex $q$. Bottom: the vertex $q$ and the angle constraint necessitate the placement of the vertex $r$. The process repeats eternally.

between the first two segments to be triangulated (Fig. 20, center), which may necessitate the placement of another vertex $q$ on the middle segment. Let $a = |pq|$ and $b = |op|$ as illustrated. If the angle bound is respected, the length $a$ is small; one can show that

$$\frac{a}{b} \leqslant \frac{\sin\phi}{\sin\theta}\left(\cos(\theta+\phi) + \frac{\sin(\theta+\phi)}{\tan\theta}\right).$$

If the upper region (above the wedge) is part of the triangulation domain, then it too must be triangulated, perhaps with the fan-like triangulation in Fig. 19. Because $T$ has no angle less than $\theta$ in the upper region, $b/a \leqslant (2\cos\theta)^{180^\circ/\theta}$. However, if the product of these bounds on $b/a$ and $a/b$ is less than one, there are no values of $a$ and $b$ that satisfy both inequalities. For any choice of $\theta > 0$, there is a choice of $\phi > 0$ for which the product of these bounds is less than one. Hence, by contradiction, there is no triangulation of such a domain in which no new angle is smaller than $\theta$.

For an angle constraint of $\theta = 30^\circ$, the bounds are incompatible when $\phi$ is about six tenths of a degree or smaller. In practice, Delaunay refinement often fails to achieve a $30^\circ$ angle bound for $\phi = 5^\circ$. A Delaunay refinement algorithm, attempting to triangulate the upper region, will introduce another vertex $r$ between $o$ and $p$ (Fig. 20, bottom). Unfortunately, the vertex $r$ creates the same conditions as the vertex $p$ in the lower region, but $r$ is closer to $o$. The process will cascade, eternally creating smaller and smaller triangles in an attempt to satisfy the angle constraint, and the algorithm will never terminate.

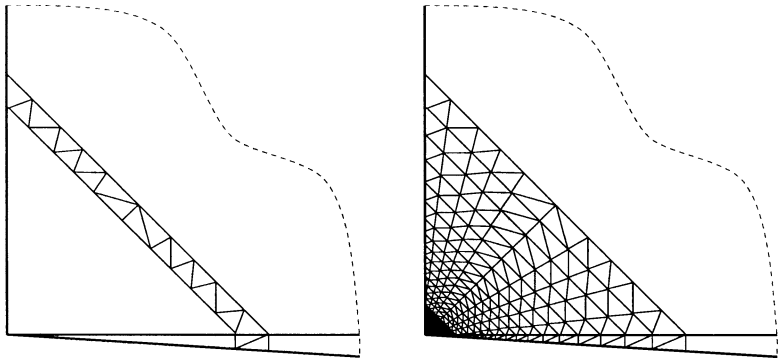

Fig. 21. How to create a quality triangulation of infinite cardinality around the apex of a very small angle. The method employs a thin strip of good-quality triangles about the vertex (left). Ever-smaller copies of the strip fill the gap between the vertex and the outer strip (right).

Oddly, it is straightforward to triangulate this PSLG using an infinite number of good-quality triangles. A vertex at the apex of a small angle can be shielded with a thin strip of good-quality triangles, as Fig. 21 illustrates. (This idea is one form of corner-lopping, discussed in the next section.) The strip is narrow enough to admit a quality triangulation in the wedge that bears the smallest input angle. Its shape is chosen so that no acute angle appears outside the shield, and the region outside the shield can be triangulated by Delaunay refinement. The region inside the shield is triangulated by an infinite sequence of similar strips, with each successive strip smaller than the previous strip by a constant factor close to one.

## 6. Practical handling of small input angles

Ruppert's algorithm fails to terminate on PSLGs like that of Fig. 20, even if the algorithm is modified so that it does not try to split any skinny triangle that bears a small input angle. As the previous section demonstrates, any mesh of such a PSLG has a small angle that is removable, but another small angle invariably takes its place. The negative result quashes all hope of finding a magic pill that will make it possible to triangulate any PSLG without introducing additional small angles. However, a practical mesh generator should always terminate, even if it must leave small angles behind. How can one detect this circumstance, and ensure termination of the algorithm while still generating good-quality triangles wherever possible?

The following sections compare a traditional solution, corner-lopping, with a new algorithm that generates better meshes in practice.

### *6.1. Corner-lopping*

Corner-lopping is an approach proposed by Bern, Eppstein, and Gilbert [5] and Ruppert [27]. The input PSLG $X$ is replaced by a modified PSLG $X'$, as Fig. 22 illustrates.

$X'$ is created by lopping off corners of $X$ where small angles lie. Any apex $a$ of a small angle (less than 60°) in $X$ is "shielded" as follows. Imagine a circle of some suitable radius centered at $a$. A radius

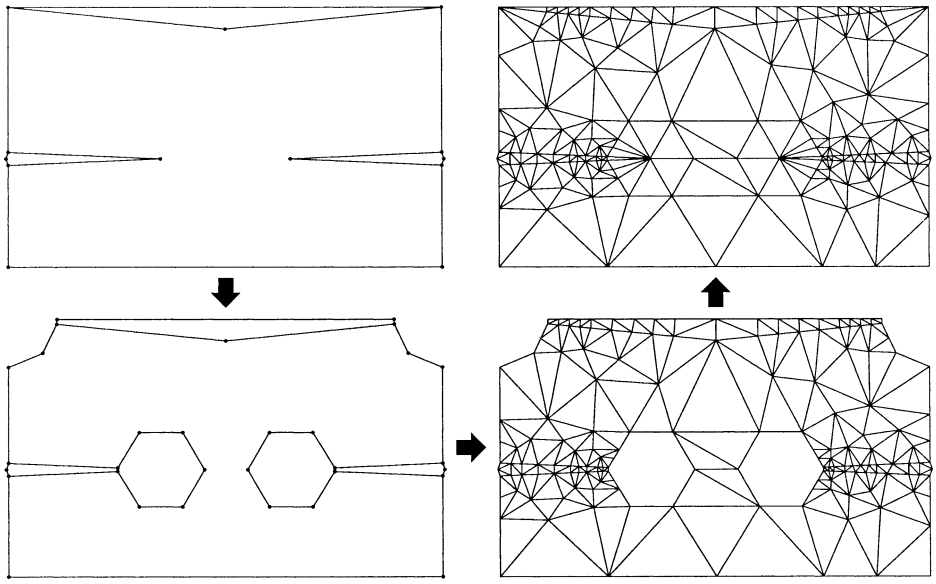

Fig. 22. A PSLG with small angles (upper left) can be triangulated by lopping off the corners where small angles appear (lower left), triangulating the modified PSLG (lower right), and filling the lopped corners with fans of triangles (upper right).

of $\mathrm{lfs}(a)/3$, where $\mathrm{lfs}(\cdot)$ is defined relative to the original PSLG $X$, is a reasonable choice. Vertices are inserted wherever the circle intersects a segment, thereby dividing the circle into arcs. If any of the arcs subtend an angle over 60° in the interior of the triangulation domain, these arcs are further divided by the insertion of additional vertices. These vertices define a convex polygon (or portion thereof) around $a$. The edges of this polygon become segments of $X'$ (which Ruppert calls *shield edges*), and the contents of this polygon are removed from the triangulation domain. Hence, $X'$ does not contain $a$, and the segments that were incident on $a$ in $X$ are shortened in $X'$.

The modified PSLG $X'$ has no small interior angles and can be triangulated using Ruppert's algorithm (as in the lower right corner of Fig. 22) or Chew's algorithm. This mesh is converted into a triangulation of the original PSLG $X$ by filling each lopped corner with a fan of triangles around each apex (adding what Ruppert calls *spoke edges*), as illustrated in the upper right corner of Fig. 22. This approach has the advantage that a new small angle can appear only at the apex of a small input angle. Ruppert [27] outlines some clever suggestions for triangulating the lopped corners with fewer new small angles. However, the negative result of Section 5 states that new small angles cannot always be avoided entirely.

An advantage of this approach is that if the minimum angle bound is $\theta \leqslant 30°$, no angle larger than $180° - 2\theta$ appears in the final mesh. Another advantage is that, if the radii of the circles are chosen carefully, corner-lopping can be implemented so that no new angle of the final mesh is smaller than the smallest input angle. (A proof of this fact would exploit the lower bounds on edge lengths given by Theorems 4 and 8, but would probably require the lopping circles to have smaller radii than $\mathrm{lfs}/3$.)

Corner-lopping is simple in concept, but somewhat troublesome to implement well. One complication is choosing the radius of the circle around each apex so as to produce the best possible mesh. A second

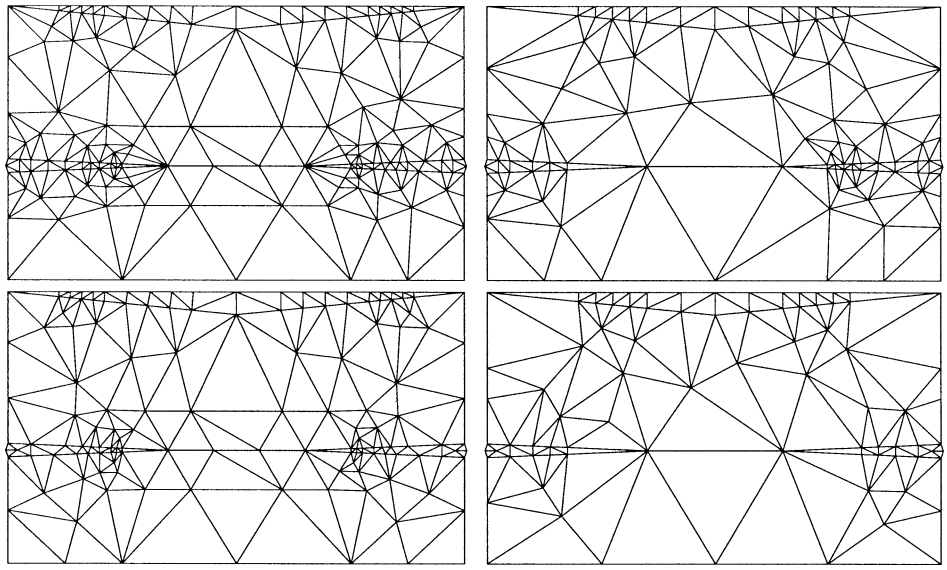

Fig. 23. Upper left: a 291-triangle mesh created by Ruppert's algorithm with corner-lopping. Upper right: a 180-triangle mesh created by the Terminator, discussed in Section 6.3. Lower left: a 246-triangle mesh created by Chew's algorithm with corner-lopping. Lower right: a 136-triangle mesh created by the Terminator with Chew-inspired diametral lenses, discussed in Section 6.4.

complication is how best to triangulate the lopped corners. To mesh them using only spoke edges gives inferior results.

The main disadvantage of corner-lopping, however, is its tendency to reduce features to a third of their original lengths. The next several sections consider an alternative approach. It is conceptually more complicated than corner-lopping, but it is no more difficult to implement, it is just as theoretically sound, and as Fig. 23 illustrates, it generally yields better meshes in practice. Observe, for instance, the shorter edges at the center of the corner-lopped meshes (left), and the larger number of small angles in the upper left mesh. In PSLGs where angles are in an intermediate range (about 10–60°), corner-lopping lops corners that might not have caused any difficulty if they had not been lopped. As we will see, the alternative approach works well in these ambiguous cases, often leaving behind no new small angles, and giving up gracefully without producing unreasonably small edges when it is not successful in eliminating all new small angles.

### *6.2. Guaranteed termination without corner-lopping*

Fig. 24 demonstrates one of the difficulties caused by small input angles. If two incident segments have unmatched lengths, an endless cycle of mutual encroachment may produce ever-shorter subsegments incident to the apex of the small angle. This phenomenon is only observed with angles of 45° or less. In these cases, the lower right cycle in the flow graph has a multiplier of $1/\sqrt{2}$ or less, and a single pair of segments causes the cycle to realize its threat of an infinite loop in the algorithm.

To solve this problem, Ruppert [27] suggests "modified segment splitting using concentric circular shells". Imagine that each input vertex is encircled by concentric circles whose radii are all the powers

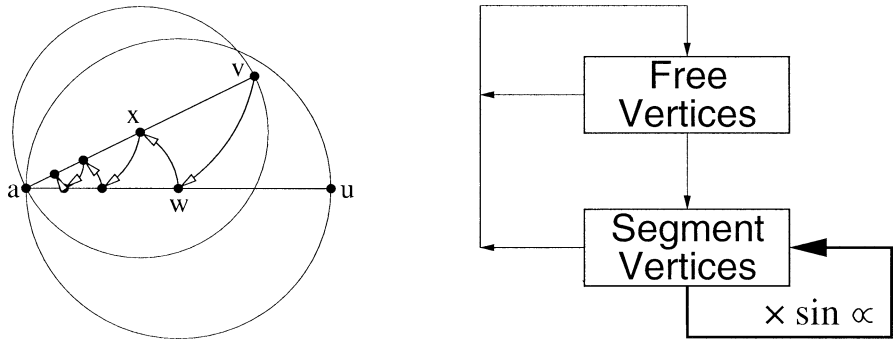


Fig. 24. Left: a problem caused by a small input angle. Vertex $v$ encroaches upon $au$, which is split at $w$. Vertex $w$ encroaches upon $av$, which is split at $x$. Vertex $x$ encroaches upon $aw$, and so on. Right: the corresponding cycle in the flow graph is shown in bold.

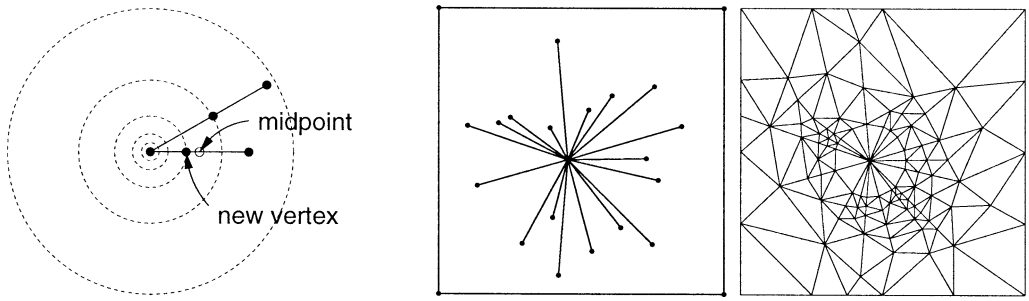


Fig. 25. Left: "modified segment splitting using concentric circular shells". If an encroached subsegment has a shared input vertex for an endpoint, the subsegment is split at its intersection with a circular shell whose radius is a power of two. Right: sample input and output of Ruppert's algorithm with concentric shell segment splitting.

of two (that is, $2^i$ for all integers $i$), as illustrated in Fig. 25. When an encroached subsegment has an endpoint that is shared with another segment, the subsegment is split not at its midpoint, but at one of the circular shells, so that one of resulting subsegments has a power-of-two length. (Clearly, the final mesh will depend on the unit of measurement chosen to represent lengths.) If both endpoints are shared, choose one endpoint's shells arbitrarily. The shell that gives the best-balanced split is chosen; in the worst case, the shorter resulting subsegment is one-third the length of the split subsegment. Each input segment may undergo up to two unbalanced splits—one for each end. All other subsegment splits are bisections.

Concentric shell segment splitting prevents the runaway cycle of ever-shorter subsegments portrayed in Fig. 24, because incident subsegments of equal length do not encroach upon each other. It tends to simulate the effects of corner-lopping, but in a lazy manner so that corners are not lopped until necessary. If Ruppert's algorithm is modified slightly so that it does not attempt to split a skinny triangle that bears a small input angle (and thus cannot be improved), concentric shell segment splitting is generally effective in practice for PSLGs that have small angles greater than about 10°, and often for smaller angles. (See Figs. 1 and 25 for examples.) It is always effective for polygons (with polygonal holes). In effect, the lower right cycle in the flow graph (Fig. 24, right) can no longer, *by itself*, cause the algorithm to fail to terminate.

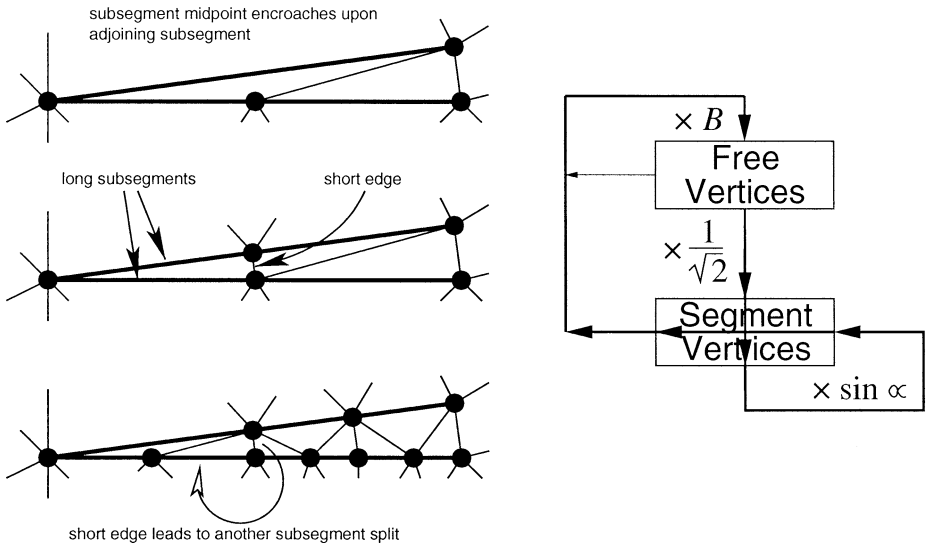


Fig. 26. Left: the short edge created opposite a small angle can cause other short edges to be created as the algorithm attempts to remove skinny triangles. If the small insertion radii propagate around an endpoint and cause the supporting subsegments to be split, a shorter edge is created, and the cycle may repeat. Right: a corresponding cycle in the flow graph is shown in bold.

However, the flow graph may contain another cycle whose product is less than one: a figure-eight loop through the flow graph (Fig. 26, right) in which a segment vertex sires another segment vertex (via a small input angle), which sires a free vertex (at the circumcenter of a skinny triangle), which sires another segment vertex. As Section 5 demonstrates, difficulties occur when a small angle is adjacent to a much larger angle. The negative result of Section 5 arises not because of the mutual encroachment problem illustrated in Fig. 24, but because the free edge opposite a small angle is much shorter than the subsegments that define the angle, as Fig. 26 (left) illustrates.

The two subsegments in Fig. 26 are coupled, in the sense that if one is bisected then so is the other, because the midpoint of one encroaches upon the other. In Ruppert's algorithm, this holds true for any two subsegments of equal length separated by 60° or less. Each time such a dual bisection occurs, a new edge is created that is shorter than the subsegments produced by the bisection; the free edge can be arbitrarily short if the angle is arbitrarily small. One of the endpoints of the free edge has a small insertion radius, though that endpoint's parent (usually the other endpoint) might have a large insertion radius. Hence, a small angle acts as an "insertion radius reducer". The new short edge will engender other short edges as the algorithm attempts to remove skinny triangles. If small insertion radii propagate around an endpoint of the short edge, the coupled subsegments may be split again, continuing an infinite sequence of shorter and shorter edges.

If the PSLG is a polygon (optionally with polygonal holes), small insertion radii cannot propagate around the short edge, because the short edge partitions the polygon into a skinny triangle (which the algorithm does not attempt to split) and everything else. The short edge is itself flipped or penetrated only if there is an even smaller feature elsewhere in the mesh. If the short edge is thus removed, the algorithm will attempt to fix the two skinny triangles that result, thereby causing the subsegments to be split again, thus creating a new shorter edge (Fig. 27).

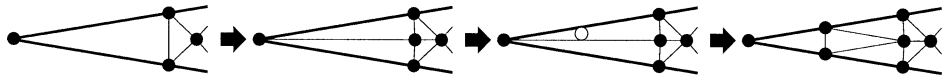

Fig. 27. Concentric shell segment splitting ensures that polygons (with holes) can be triangulated, because it causes small angles to be clipped off. This sequence of illustrations demonstrate that if a clipped triangle's interior edge is breached, a smaller clipped triangle will result.

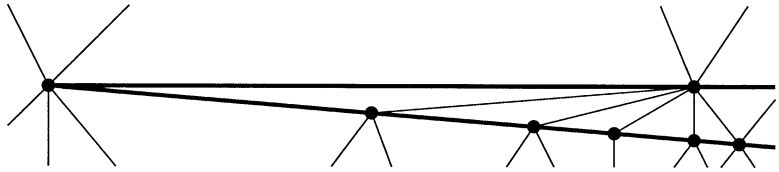

Fig. 28. The simplest method of ensuring termination when small input angles are present has undesirable properties, including the production of large angles and many small angles.

For general PSLGs, how may one diagnose and cure cycles of diminishing edge lengths? A sure-fire way to guarantee termination is to never create an edge shorter than $\mathrm{lfs}_{\min}$. Here's an example of a strategy that achieves this goal while still accounting for mesh grading: never insert a vertex whose insertion radius is smaller than the insertion radius of its most recently inserted ancestor (its parent if the parent was inserted; its grandparent if the parent was rejected), unless its parent is an input vertex or lies on a nonincident segment.

This cure works by directly attacking the lower right cycle in the flow graph of Fig. 26. When the cycle's multiplier is smaller than one, the child vertex is simply not inserted. The precise rule is that if a subsegment is encroached upon by a segment vertex, and the new vertex inserted in the encroached subsegment would have a smaller insertion radius than the encroaching vertex, do not split the encroached subsegment.

This restriction is undesirably conservative for two reasons. The first problem is demonstrated in Fig. 28. Two subsegments are separated by a small input angle, and one of the two is bisected. The other subsegment is encroached, but is not bisected because its midpoint would have a small insertion radius. One unfortunate result is that the triangle bearing the small input angle also has a large angle of almost $180^\circ$. Large angles can be worse than small angles, because they jeopardize interpolation accuracy and convergence of the finite element method in ways that small angles do not. Another unfortunate result is that other skinny triangles may form. The skinny triangles in the figure cannot be improved without splitting the upper subsegment.

Second, if subsegments remain encroached, the mesh is unsuitable for applications that require the final triangulation to be truly Delaunay, or that (like some finite volume methods) require all triangle circumcenters to lie in the triangulation.

### *6.3. A better algorithm: the Terminator*

As an alternative, I suggest a Delaunay refinement algorithm called the *Terminator*, which produces fewer large angles in practice than the simple solution described above, and offers guaranteed termination and a guaranteed minimum angle.

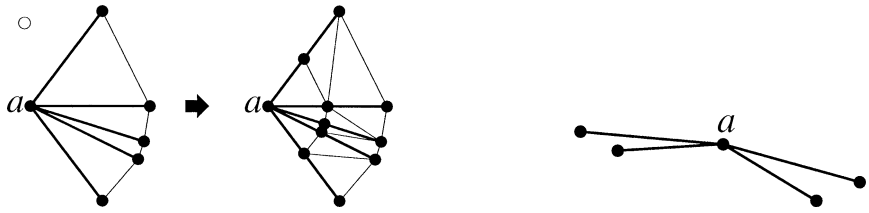


Fig. 29. (a) Example of a subsegment cluster. If all the subsegments of a cluster have power-of-two lengths, then they all have the same length and are effectively split as a unit because of mutual encroachment. (b) Several independent subsegment clusters may share the same apex.

The Terminator is based on Delaunay refinement with concentric shell segment splitting and a look-ahead procedure that prevents unsafe subsegment splits. When a subsegment $s$ is encroached upon by the circumcenter of a skinny triangle, a decision is made whether to split $s$ with a vertex $v$, or to leave $s$ whole. (In either case, the circumcenter is rejected.) The decision process is somewhat elaborate.

If neither endpoint of $s$ bears an input angle of 60° or less, or if both endpoints do, then $s$ is split. (If every input angle is greater than 60°, the Terminator acts no differently than Ruppert's algorithm.) Otherwise, let $a$ be the apex of the small angle. Define the *subsegment cluster* of $s$ to be the set of subsegments incident to $a$ that are separated from $s$, or from some other member of the subsegment cluster of $s$, by 60° or less. (However, "exterior" small angles are ignored; two subsegments are not necessarily part of the same cluster if the region between them is not part of the triangulation domain.) Once all the subsegments of a cluster have been split to power-of-two lengths, they must all be the same length to avoid encroaching upon each other. If one is bisected, the others follow suit, as illustrated in Fig. 29(a).

Not all subsegments incident to an input vertex are necessarily part of the same cluster. For instance, Fig. 29(b) shows two independent subsegment clusters sharing one apex, separated from each other by angles over 60°.

Let $t$ be a skinny or oversized triangle whose circumcenter encroaches upon a subsegment $s$ that belongs to a subsegment cluster. Let $v$ be the vertex that will be introduced if $s$ is split. Let $g$ be $v$'s grandparent (and the parent of $t$'s circumcenter). The Terminator determines the insertion radius $r_g$ of $g$ and the minimum insertion radius $r_{\min}$ of all the subsegment vertices (including $v$) that will be introduced into the subsegment cluster of $s$ if all the subsegments in the cluster are split to a length of $|s|/2$. This radius is the length of the shortest free edge that will appear opposite a small angle of the subsegment cluster, so $r_{\min} = |s|\sin(\phi_{\min}/2)$, where $\phi_{\min}$ is the smallest angle separating two subsegments of the cluster.

The vertex $v$ is inserted, splitting $s$, if and only if one or more of the following six conditions hold.

A. $r_{\min} \geqslant r_g$;
B. the triangle $t$ is too large (according to some user-defined criterion);
C. the length of $s$ is not a power of two;
D. $s$ has two subsegment clusters—one at each endpoint;
E. some subsegment in the subsegment cluster of $s$ is shorter than $s$; or
F. no ancestor of $v$ lies in the relative interior of the segment containing $s$. (It is not relevant whether an endpoint of the segment is an ancestor of $v$.)

Condition A permits subsegment splits that do not engender shorter edges than the existing edges. The remaining five conditions are optional heuristics that help improve the mesh by allowing shorter edges to be created in specific circumstances, without threatening the termination guarantee. Condition B ensures that all oversized triangles are eliminated. Conditions C, D, and E help to create isosceles triangles (which are the best we can hope for) at small input angles. Condition F attempts to distinguish between the case where a subsegment is encroached because of small input features, and the case where a subsegment is encroached because it bears a small input angle. Any of the last five conditions can be omitted, but C, D, and E are strongly recommended. Be aware that Condition F may significantly slow down the algorithm if the chains of vertex ancestors grow long.

If the Terminator declines to insert $v$, and no subsegment is split because of encroachment by the circumcenter of $t$, the Terminator never again tries to split $t$. See Appendix A for details.

**Theorem 11.** *The Terminator always terminates.*

**Proof.** If $r_{\min} < r_g$, but $v$ is inserted in $s$ anyway because one of the other five conditions hold, $v$ is called a *trigger vertex,* because it (usually) triggers the splitting of all the subsegments in a cluster and thereby creates a new edge whose length $r_{\min}$ is less than $r_g$. A trigger vertex is named according to the condition that allows its insertion; for example, a *Type C trigger vertex* is inserted because the length of $s$ is not a power of two. Recall that the parent of any trigger vertex is a rejected circumcenter of a skinny or oversized triangle, and bad triangles have lower priority than encroached subsegments, so a trigger vertex is only generated when no subsegment in the mesh is encroached upon by a mesh vertex.

Say that a vertex $v$ is a *diminishing vertex* if its insertion radius $r_v$ is less than that of all its ancestors. It is a consequence of Lemma 3 that if $v$ is a diminishing vertex, $v$ must have been inserted in a subsegment $s$ in one of the following circumstances.

(1) $v$ is not the midpoint of $s$, because $s$ was split using concentric circular shells;
(2) $s$ is encroached upon by an input vertex, or by a vertex lying on a segment not incident to the segment that contains $s$; or
(3) $s$ is encroached upon by a vertex $p$ that lies on a segment incident to $s$ at an angle less than 60°. Clearly, the insertion of $v$ was preceded by the insertion of either a trigger vertex or one of the above two types of diminishing vertices in the same subsegment cluster.

Call these Type 1, 2, and 3 diminishing vertices, respectively.

The rest of the proof will show that only a finite number of Types B–F trigger vertices and Types 1–3 diminishing vertices can be inserted. After the last diminishing vertex is inserted, no edge ever appears whose length is less than the minimum insertion radius of all the diminishing vertices and input vertices. Because this establishes a lower bound on edge lengths, the Terminator terminates; it must eventually run out of places to put new vertices.

The total number of diminishing vertices of Type 1, plus trigger vertices of Type C or D, is at most twice the number of segments in the PSLG. After a segment undergoes two off-center splits, the subsegments at the ends of the segment have power-of-two lengths.

Only a finite number of Type 2 diminishing vertices can be inserted, because any subsegment shorter than $\mathrm{lfs}_{\min}$ cannot be encroached upon by a nonincident feature.

By Lemma 3, a Type B trigger vertex cannot split a subsegment to a length shorter than the circumradius of the bad triangle divided by $\sqrt{2}$. Any reasonable definition of “oversized” applies only

to triangles whose circumradii are above some positive threshold. Hence, once the subsegments in every cluster are sufficiently short, no more Type B trigger vertices can be inserted.

No Type F trigger vertex is ever inserted in the relative interior of the same segment as any of its ancestors, so each input segment may contain at most one Type F trigger vertex for each input vertex.

Finally, we come to Type 3 diminishing vertices and Type E trigger vertices, which are inserted into a subsegment only if there is some shorter subsegment in the same cluster. How did that subsegment get to be shorter? Consider a subsegment cluster whose shortest original segment has a length of at least $2^{i+2}$ for some integer $i$. Thanks to concentric shell segment splitting, once a subsegment in this cluster has been split to a length of $2^i$ or smaller, its length is a power of two. If a subsegment of this cluster whose length is $\ell \leqslant 2^i$ is split by the insertion of a Type 3 or Type E vertex, the cluster must have already contained a subsegment of length $\ell/2$. Therefore, a subsegment that is shorter than the shortest subsegment in the same cluster (and shorter than $2^i$) cannot be created by inserting a Type 3 or Type E vertex.

It follows that only a finite number of Type 3 diminishing vertices and Type E trigger vertices can be inserted for each diminishing vertex or trigger vertex of another type inserted. Therefore, the Terminator inserts only a finite number of diminishing vertices, and it is guaranteed to terminate. □

**Theorem 12.** *Let $\phi$ be the smallest angle of a PSLG, with $\phi \leqslant 60°$. The Terminator produces a mesh of the PSLG wherein every triangle has a circumradius-to-shortest edge ratio no greater than* $1/[\sqrt{2}\sin(\phi/2)]$. (*Note that for $\phi = 60°$, this bound is $\sqrt{2}$, matching the bound for PSLGs free of acute angles.*) *Hence, no angle of the final mesh is less than* $\arcsin[\sin(\phi/2)/\sqrt{2}]$.

**Proof.** Let $t$ be a skinny triangle that is not eliminated by the Terminator, as illustrated in Fig. 30. $t$ is not split because its circumcenter $p$ encroaches upon a subsegment $s$ whose splitting would have split a subsegment cluster, yielding a short edge of length $r_{\min}$ opposite the apex of the cluster. Let $v$ be the midpoint of $s$; $p$ would be the parent of $v$ if $v$ had been inserted. Let $g$ be the parent of $p$ (and the grandparent of $v$). Let $d$ be the length of $t$'s shortest edge. Recall that $r_p$ is the circumradius of $t$, so $r_p/d$ is $t$'s circumradius-to-shortest edge ratio.

Because $g$ is the most recently inserted endpoint of $t$'s shortest edge (by the definition of "parent"), $r_g \leqslant d$. Because the Terminator chose not to insert $v$, $r_{\min} < r_g$. By Lemma 3, $r_p \leqslant \sqrt{2}\,r_v$. If the subsegment cluster of $s$ had been split, every resulting subsegment would have length $r_v$. If the smallest

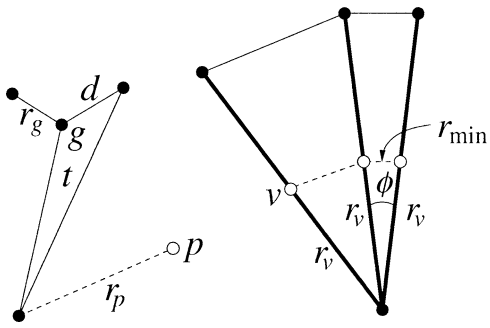


Fig. 30. If the Terminator does not split $t$, the smallest angle of *t is* not much smaller than $\phi$.

angle of the subsegment cluster of $s$ is $\phi$, basic trigonometry shows that $\sin(\phi/2) = r_{\min}/(2r_v)$. Putting these inequalities together, the circumradius-to-shortest edge ratio of $t$ is $r_p/d < 1/[\sqrt{2}\sin(\phi/2)]$. □

The Terminator eliminates all encroached subsegments, and is suitable for applications that require the final mesh to be Delaunay and have every triangle's circumcenter in the mesh. Because subsegments are not encroached, an angle near 180° cannot appear immediately opposite a subsegment (as in Fig. 28), although large angles can appear near subsegment clusters.

Skinny triangles in the final mesh occur only near input angles less than (in practice, *much* less than) 60°. What does "near" mean? Every skinny triangle's circumcenter encroaches upon a subsegment cluster bearing a small input angle. Because $\arcsin[\sin(\phi/2)/\sqrt{2}] \sim \phi/(2\sqrt{2})$ for small $\phi$, the smallest angle in the final mesh cannot be smaller than the smallest input angle by a factor of much more than $2\sqrt{2}$. This bound is not quite as good as the bound of $\phi$ that corner-lopping, carefully implemented, can achieve. However, the Terminator performs better than corner-lopping in practice, and angles smaller than $\phi$, while theoretically possible, have not been observed.

### 6.4. Terminator Chew

Chew's algorithm and the Terminator can be combined straightforwardly, as each of them can be viewed as a modification to Ruppert's algorithm. However, the combined algorithm is unsatisfactory. Suppose that a segment $s$ is encroached, but the Chew–Terminator combination declines to split $s$, following the rules of Section 6.3. Should the free vertices inside the diametral circle of $s$ be deleted anyway? If they are deleted, the combination algorithm may fail to terminate, because vertices are eternally created and deleted in the diametral circle; see Fig. 31 for an example. If they are not deleted, arbitrarily skinny triangles may survive, like $t$ in Fig. 31. The bound on the smallest angle established by Theorem 12 does not apply to the Chew–Terminator because it is not possible to bound the circumradius of the worst triangle. For example, the circumradius of $t$ in Fig. 31 can be arbitrarily large. (The Ruppert–Terminator's bound on circumradius, from Theorem 12, does not transfer to Chew's algorithm because Lemma 5 changes the definition of "parent".)

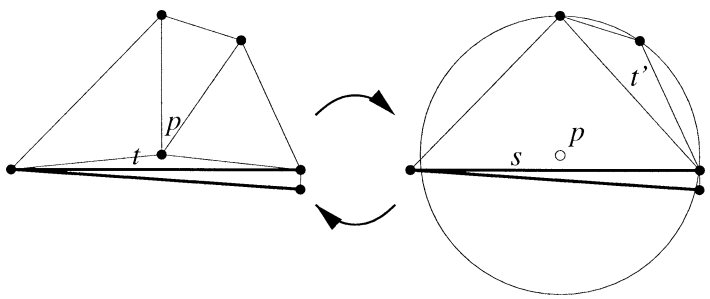


Fig. 31. Chew's algorithm wants to split the skinny triangle $t$, but the circumcenter of $t$ lies on the other side of $s$, so $s$ is encroached. The Terminator declines to split $s$, so that a shorter edge is not created. Should vertices inside the diametral circle of $s$ be deleted? If not, an arbitrarily bad triangle $t$ will survive. If the vertices are deleted, the algorithm may fail to terminate. In this example, when $t'$ is split, the triangle $t$ is recreated, and an infinite loop occurs.

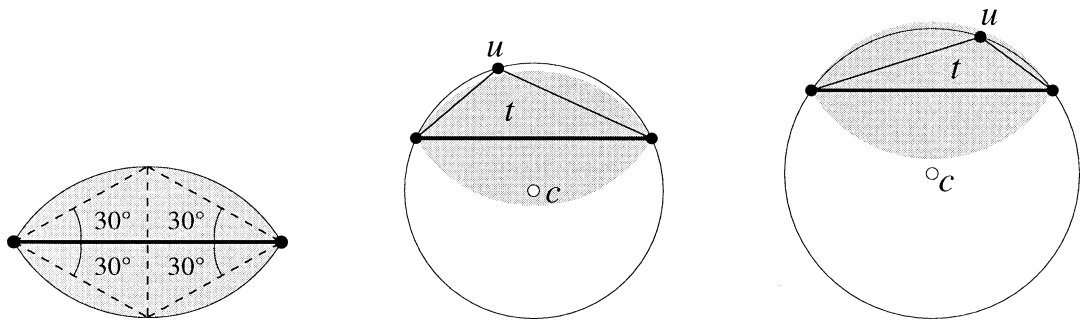


Fig. 32. (a) A hybrid Chew–Ruppert algorithm uses diametral lenses. Any vertex in the shaded region encroaches upon this subsegment. (b, c) If a skinny triangle and its circumcenter lie on opposite sides of a subsegment, then either the circumcenter of or a vertex of the triangle lies in the subsegment's diametral lens.

To rescue the combination algorithm, change the definition of encroachment. Replace Ruppert's diametral circles with *diametral lenses*, illustrated in Fig. 32(a). The diametral lens of a subsegment $s$ is the intersection of two disks whose centers lie on the bisector of $s$, with one center on each side of $s$. Each disk's center is at a distance of $|s|/(2\sqrt{3})$ from $s$, where $|s|$ is the length of $s$. Each disk has radius $|s|/\sqrt{3}$, so each disk's boundary passes through the endpoints of $s$ and the center of the other disk. As Fig. 32(a) shows, a diametral lens is just big enough to accommodate an isosceles triangle whose base is $s$ and whose angles at the base are 30°.

Much like in Ruppert's algorithm, a subsegment $s$ is encroached if there is a vertex, or if a vertex is rejected for insertion, in the diametral lens of $s$ (including its boundary), unless another subsegment obstructs the visibility of the encroaching vertex from the interior of $s$. A vertex considered for insertion at the circumcenter of a skinny triangle is rejected if it lies in the diametral lens of a subsegment, and the subsegment is split instead. As in Chew's algorithm, all free vertices that are inside the diametral circle of $s$ and visible from the midpoint of $s$ are deleted before $s$ is bisected.

Any segment encroached in Chew's algorithm also has an encroached diametral lens (but the reverse is not necessarily true); and any segment whose diametral lens is encroached also has an encroached diametral circle (but the reverse is not necessarily true). The latter statement is obvious, but let's examine the former one. Let $t$ be a skinny triangle whose circumcenter $c$ lies on the opposite side of a subsegment $s$. Let $u$ be any vertex of $t$ that is not an endpoint of $s$. Obviously, $u$ is on the circumcircle of $t$. There are two possibilities: either $c$ encroaches upon the diametral lens of $s$, as in Fig. 32(b), or $u$ encroaches upon the diametral lens, as in Fig. 32(c).

Because lens-based encroachment lies between Ruppert's and Chew's algorithms in its aggressiveness in splitting subsegments, it is not surprising that its angle bound lies between their bounds as well. Let $p$ be a circumcenter that is rejected because it encroaches upon the diametral lens of a subsegment $s$, and let $v$ be the vertex inserted at the midpoint of $s$. If "parent" is defined as for Ruppert's algorithm, $p$ is the parent of $v$. Because diametral lenses are narrower than diametral circles, a better bound is available for the insertion radius of $v$ than in Ruppert's algorithm. The bound is $r_v \geqslant r_p \cos 30° = (\sqrt{3}/2)r_p$, and the proof is much like that of the related bound in Lemma 3. The limiting case, where $r_v = (\sqrt{3}/2)r_p$, occurs when $p$ lies on the topmost or bottommost point of the lens depicted in Fig. 32(a).

In Fig. 17, replace the multiplier "$\times \cos\theta$" with "$\times\sqrt{3}/2$". If no input angle is smaller than 60°, this Ruppert–Chew hybrid terminates if $B \geqslant 2/\sqrt{3}$, giving an angle bound of up to $\arcsin(\sqrt{3}/4) \doteq 25.65°$, which is not quite as good as the 26.56° bound of Chew's algorithm, but is still better than the 20.7° bound of Ruppert's algorithm.

If a circumcenter $p$ encroaches upon the diametral lens of a subsegment $s$, but the Terminator declines to split $s$, then $p$ is rejected (not inserted), but other vertices inside the diametral circle of $s$ are *not* deleted. This way, termination can still be guaranteed, but $s$ cannot take part in an arbitrarily skinny triangle. In Fig. 31, the right-hand configuration is preferred.

Several other ways in which the Terminator interacts with diametral lenses merit some scrutiny. The definition of "subsegment cluster" in Section 6.3 is motivated in part by the fact that if all the subsegments in a cluster have equal length, and one is split, then all the subsegments are split by mutual encroachment. When diametral lenses replace diametral circles, this statement holds true only if the subsegments are separated by angles of $\arctan\sqrt{13/3} - 30° \doteq 34.34°$ or less. However, subsegment clusters are still defined by a 60° angle, because any angle less than 60° still functions as an "insertion radius reducer".

Theorem 11 (which guarantees that the Terminator terminates on any PSLG) also applies when diametral lenses are used. The bound on the smallest new angle, derived in Theorem 12, can be improved by using the bound $r_v \geqslant (\sqrt{3}/2)r_p$. If the smallest angle in the input PSLG is $\phi \leqslant 60°$, the mesh produced by the Terminator with diametral lenses has no angle smaller than $\arcsin[(\sqrt{3}/2)\sin(\phi/2)] \sim (\sqrt{3}/4)\phi$.

### 6.5. *Sample meshes*

Fig. 33 depicts a PSLG with nine small angles ranging from 1.43° to 8.97°, two meshes thereof produced by the Terminator using diametral circles (top), and two meshes produced by the Terminator using diametral lenses (bottom). The left meshes were produced with an angle bound of 20.7°, and the right meshes with an angle bound of 33°.

The upper left mesh has nine new angles less than 20.7°, of which two are less than 10° and the smallest is 5.83°. The lower left mesh has five new angles less than 20.7°, of which only the smallest, 6.24°, is less than 10°. The upper right mesh has 111 new angles less than 33°, of which twelve are less than 10° and the smallest is 5.83°. The lower right mesh has 86 new angles less than 33°, of which nine are less than 10° and the smallest is 4.49°. The original version of Ruppert's algorithm fails on this PSLG with any angle bound larger than about 11.5°, and Chew's algorithm fails for angle bounds larger than about 13°. (They terminate for smaller angle bounds only if they use concentric circular shells to split subsegments.)

The advantages of diametral lenses over diametral circles are most boldly realized when there are many small input angles or long, closely-spaced parallel segments, because lenses cause adjacent segments to encroach upon each other to a lesser degree than diametral circles do. As a consequence, fewer triangles are produced.

The program that produced these meshes deviates from the algorithm discussed in Sections 6.3 and 6.4 in two ways. First, because of time limitations (and to save memory), Condition F was not implemented.

The second difference is a slight simplification of Condition A, which saves a little bit of memory and programming effort. The Terminator needs to know the insertion radius of a vertex only when it considers inserting a vertex $v$ into a subsegment cluster. It is straightforward to compute the insertion radii of $v$ and the other vertices that will be inserted into the cluster. However, the insertion radius of $v$'s grandparent $g$ cannot be determined by inspecting the current mesh, because other vertices may have been inserted

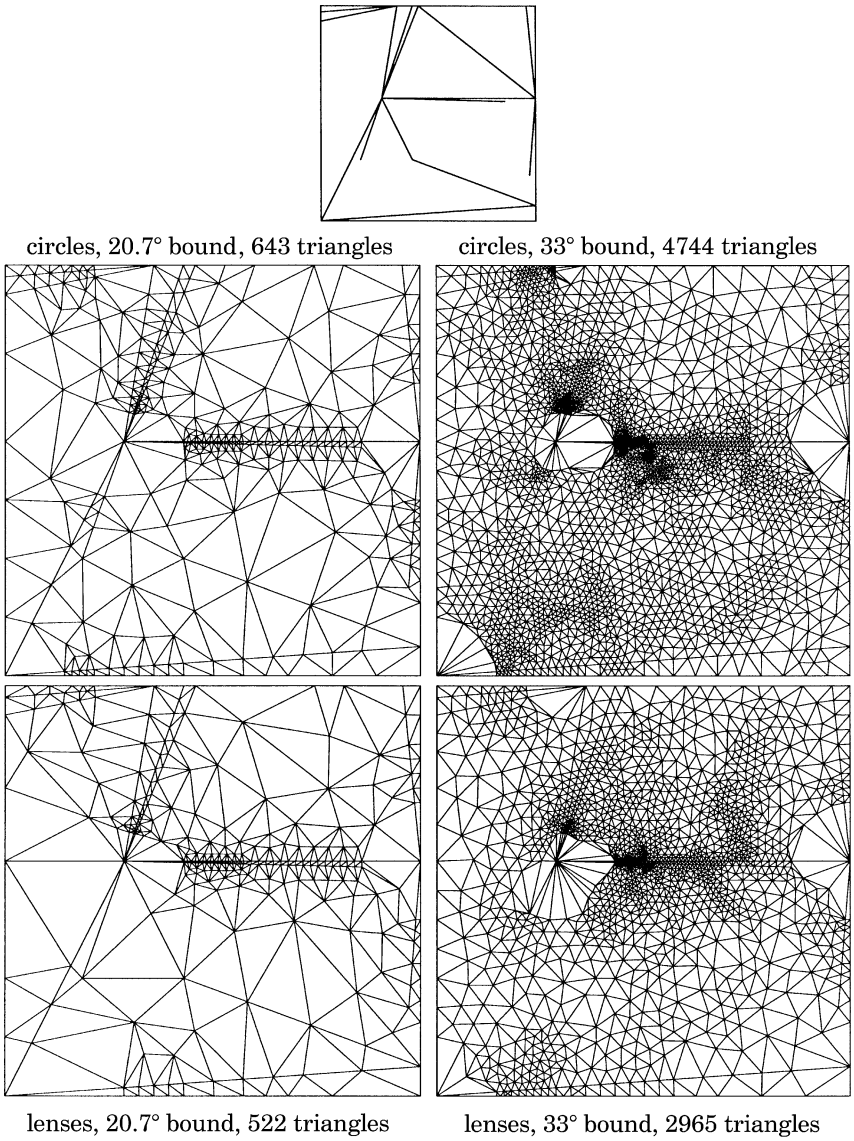


Fig. 33. Four meshes of a PSLG (top) produced by the Terminator. The top two meshes were created using diametral circles to define encroachment, and the bottom two were created using diametral lenses. The left meshes were produced with an angle bound of 20.7°; the right meshes with a bound of 33°. Angles smaller than these bounds occur only in triangles whose circumcenters would encroach upon a subsegment cluster.

near $g$ since $g$ was inserted. Nevertheless, a good substitute for $r_g$ is the length $d$ of the shortest edge of the skinny triangle whose circumcenter is $v$'s parent, illustrated in Fig. 30. The length $d$ is an upper bound on $r_g$, so its use will not jeopardize the Terminator's termination guarantee; the modified algorithm is more conservative in its decision about whether to insert $v$. The Terminator's minimum angle bound (Theorem 12) still holds as well. With this modification, there is no need to store the insertion radius of

each vertex, nor to store the information needed to determine which of the endpoints of an edge was most recently inserted.

## 7. Extensions and improvements

Here, I describe several twists to the Delaunay refinement algorithms. The first extends them to flat interlocking surfaces embedded in three-dimensional space. The second improves the quality of triangles away from the boundary of the mesh. The third, which generalizes an idea of Chew, improves the quality of triangles everywhere.

### *7.1. Meshing adjoining planar surfaces in three dimensions*

Applications such as global illumination and radiosity use surface meshes of three-dimensional objects for lighting calculations and interpolation. A Delaunay refinement algorithm can mesh each planar surface independently, but what if the surfaces adjoin each other at shared edges, and the triangulations are required to conform to each other—that is, match triangle edge to triangle edge—along their shared boundaries?

Surprisingly, the Delaunay refinement algorithms need no conceptual changes to tackle this problem, so long as all the surfaces can be meshed simultaneously. The key is to redefine the notion of local feature size to use geodesic distances, rather than straight-line distances.

As a prelude, consider the significance of geodesic distances for triangulations of nonconvex two-dimensional domains. Delaunay refinement algorithms begin by forming a constrained Delaunay triangulation of the input PSLG. As Fig. 34 (left) shows, if Delaunay refinement is performed before exterior triangles (those that are not part of the triangulation domain) are removed, overrefinement can occur near small exterior features. Overrefinement is prevented if exterior triangles are removed before refinement begins, and the encroachment of a subsegment by a vertex on its exterior side is ignored, as illustrated in Fig. 34 (right).

Ruppert [27] points out that the difference between these two cases can be formalized by redefining "local feature size". Let the *geodesic distance* between two points be the length of the shortest path

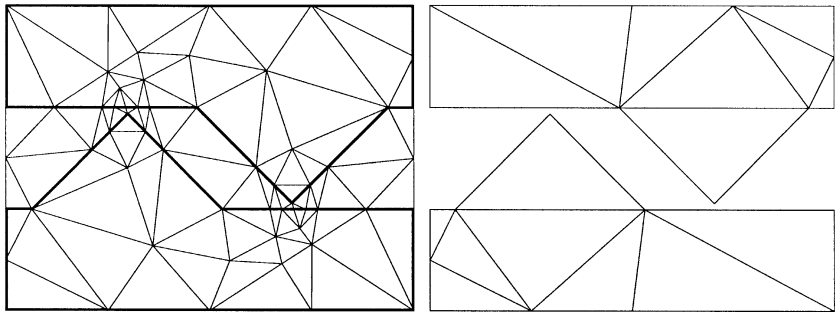

Fig. 34. Two variations of Ruppert's Delaunay refinement algorithm with a 20° minimum angle. Left: if Delaunay refinement is performed before exterior triangles are removed, overrefinement can occur. Right: mesh created by removing exterior triangles before refinement.

between them that lies entirely in the triangulation domain. In other words, any geodesic path must go around holes and concavities. Given a PSLG $X$ and a point $p$ in the triangulation domain of $X$, define the local feature size $\mathrm{lfs}(p)$ to be the smallest value such that there exist two points $u$ and $v$ within a geodesic distance of $\mathrm{lfs}(p)$ from $p$ that lie on features (vertices or segments) of $X$ that are not incident to each other. This is essentially the same as the definition of local feature size given in Section 3.2, except that Euclidean distances are replaced with geodesic distances.

All of the proofs in this article can be made to work with geodesic distances. Lemma 2 depends only upon the triangle inequality, which holds for geodesic distances as well as Euclidean distances. Lemmata 3 and 5 hold because a child and its parent cannot be separated by an untriangulated region of the plane; they are visible to each other. The geodesic definition of local feature size prevents small exterior feature separations from influencing local feature sizes. Theorem 8's bounds on edge lengths are thus sometimes improved: in the left mesh of Fig. 34, edge lengths are proportional to Euclidean local features sizes, whereas in the right mesh, edge lengths are proportional to geodesic feature sizes.

These observations about geodesic distance extend directly to planar surfaces embedded in three (or more) dimensions, which may join each other along shared segments. The triangulation domain is the union of all the planar surfaces. The geodesic distance between two points is the length of the shortest path between them that lies entirely within the triangulation domain. Where surfaces meet at shared segments, features in one surface may affect the local feature size in another, reflecting the fact that the refinement of one surface can affect another surface by splitting the shared segments.

The Delaunay refinement algorithms discussed in this article may be applied in this context with essentially no conceptual changes. There are some interesting implications, however; for instance, subsegment clusters need not be planar. An arbitrary number of planar surfaces might intersect at a single segment, and in each of these surfaces, the segment might participate in a small angle. However, the termination proofs require no change to account for this.

### *7.2. Improving the quality bound in the interior of the mesh*

A simple improvement arises easily from the discussion in Section 3.3. So long as no cycle having a product less than one appears in the insertion radius flow graph (Fig. 13 or 17), termination is assured. The barrier to reducing the quality bound $B$ below $\sqrt{5}/2$ is the fact that, when an encroached segment is split, the child's insertion radius may be a factor of $\sqrt{5}/2$ smaller than its parent's. However, not every segment bisection is a worst-case example, and it is easy to explicitly measure the insertion radii of a parent and its potential progeny before deciding to take action. One can take advantage of these facts with either of the following strategies.

- Use a quality bound of $B = 1$ for triangles that are not in contact with segment interiors, and a quality bound of $B = \sqrt{2}$ (for Ruppert's algorithm) or $B = \sqrt{5}/2$ (for Chew's second algorithm) for any triangle having a vertex that lies in the interior of a segment.
  This strategy is easily understood from Fig. 35. Because segment vertices may have smaller insertion radii than free vertices, segment vertices are only allowed to father free vertices whose insertion radii are larger than their own by a factor of $\sqrt{2}$ or $\sqrt{5}/2$, as appropriate. Hence, no diminishing cycles are possible.
- Attempt to insert the circumcenter of any triangle whose circumradius-to-shortest edge ratio is larger than one. If any subsegments would be encroached, the circumcenter is rejected as usual, and each encroached subsegment is checked to determine the insertion radius of the new vertex that might be

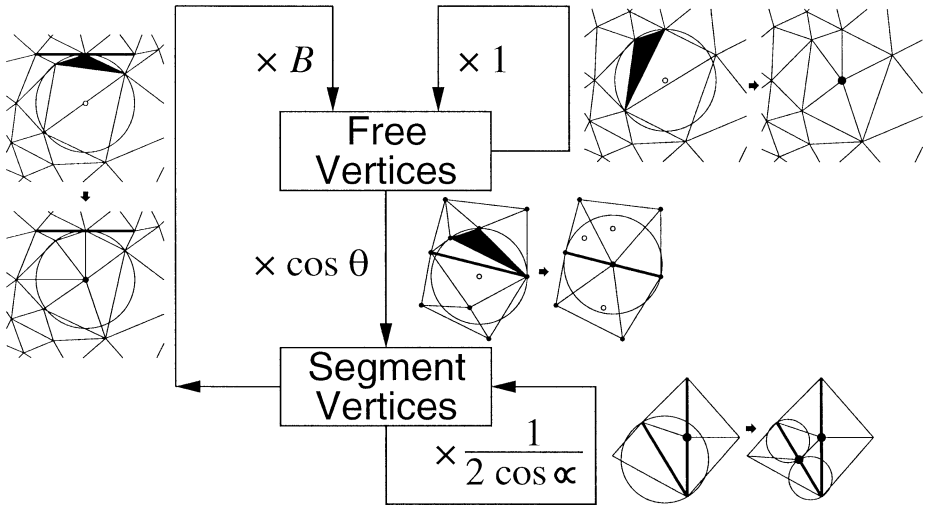


Fig. 35. This flow diagram demonstrates how a simple modification to Chew's (or Ruppert's) algorithm can improve the quality of triangles away from mesh boundaries.

inserted at its midpoint (which is half the length of the subsegment). The only midpoints inserted are those whose insertion radii are at least as large as the length of the shortest edge of the skinny triangle. This strategy works for the same reason the Terminator works: mesh vertices are expressly forbidden from creating descendants having insertion radii smaller than their own.

The first strategy differs from the second in its tendency to space segment vertices more closely than free vertices. The second strategy tends to space segment vertices and free vertices somewhat more equally. The first strategy interrupts the propagation of reduced insertion radii from segment vertices to the free vertices, whereas the second interrupts the process by which free vertices create segment vertices with smaller insertion radii. The effect of the first strategy is easily stated: upon termination, all angles are better than 20.7° (for Ruppert's algorithm) or 26.5° (for Chew's), and all triangles whose vertices do not lie in segment interiors have angles of 30° or better. For the second strategy, the delineation between 26.5° triangles and 30° triangles is not so simply stated, although the former only occur near segments.

If the angle bounds of the first strategy are loosened, the algorithm still exhibits good grading and size optimality. Bounds similar to those derived in Section 4.3 can be obtained, but the exercise is not especially enlightening, so details are omitted here.

### *7.3. Range-restricted segment splitting*

Chew's second Delaunay refinement algorithm, as he originally presented it [10], applies a quality bound of $B = 1$ to all triangles of the mesh, so no angle is smaller than 30°. He achieves this bound through the occasional use of off-center segment splits. This section generalizes Chew's idea so that it can be applied to Ruppert's algorithm and both versions of the Terminator as well. When the angle bound is 30°, however, there is no accompanying guarantee of good grading or size optimality. The modification is completely unnecessary in practice—Ruppert's and Chew's algorithms consistently achieve angle bounds better than 30° without it—but it is of theoretical interest, and it completes the presentation of Chew's second Delaunay refinement algorithm.

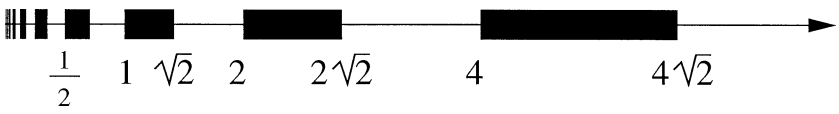


Fig. 36. Legal subsegment lengths are of the form $c2^x$, where $c \in [1, \sqrt{2})$ and $x$ is an integer.

Consider Ruppert's algorithm first. Observe that the only mechanism by which a vertex can have a child with a smaller insertion radius than its own is by encroaching upon a subsegment. By Lemma 3, an encroaching circumcenter $v$ cannot have a child whose insertion radius is smaller than $r_v/\sqrt{2}$ (if all subsegment splits are bisections), and hence it cannot cause the splitting of a segment whose length is less than $\sqrt{2}r_v$. Hence, a vertex $v$ can only produce a child whose insertion radius is less than $r_v$ if a segment is present whose length is between $\sqrt{2}r_v$ and $2r_v$. If no such segment exists, the cycle of diminishing edge lengths is broken.

Thus the motivation for *range-restricted segment splitting.* Whenever possible, the length of each subsegment is restricted to be of the form $c2^x$, where $c \in [1, \sqrt{2})$ and $x$ is an integer. This restriction is illustrated in Fig. 36, wherein darkened boxes on the number line represent legal subsegment lengths. The positive reals are partitioned into contiguous sets, each having a geometric width of $\sqrt{2}$, and alternate sets are made illegal. With this choice of partition, the bisection of any legal subsegment will produce legal subsegments.

Of course, input segments might not have legal lengths. However, when an encroached segment of illegal length is split, rather than place a new vertex at its midpoint, one may place the vertex so that the resulting subsegments fall within the legal range.

How does this restriction help? Assume no input angle is less than $45°$. Then a vertex whose insertion radius is $2^x$ or greater for some integer $x$ cannot have a descendant whose insertion radius is less than $2^x$ unless a subsegment having illegal length is split. However, each illegal subsegment can be split only once, yielding subsegments of legal length; hence, the fuel for diminishing edge lengths is in limited supply.

An illegal segment of the form $c2^x$, where $c \in [\sqrt{2}, 2)$ and $x$ is an integer, is split into subsegments of lengths $c_1 2^x$ and $c_2 2^x$ as follows.

- If $c \in [\sqrt{2}, \frac{3}{2})$, then $c_1 = \frac{\sqrt{2}}{4} - \varepsilon$ and $c_2 = c - c_1$. (Here, $\varepsilon$ is a minuscule value used because $\frac{\sqrt{2}}{4}$ is technically not in the legal range. In practice, let $c_1$ be the largest floating-point number less than $\frac{\sqrt{2}}{4}$.)
- If $c \in [\frac{3}{2}, 1 + \frac{\sqrt{2}}{2})$, then $c_1 = 1$ and $c_2 = c - c_1$.
- If $c \in [1 + \frac{\sqrt{2}}{2}, 2)$, then $c_1 = \frac{\sqrt{2}}{2} - \varepsilon$ and $c_2 = c - c_1$.

The most unbalanced split occurs if $c$ is just slightly less than $3/2$. Then, the ratio between $c_1$ and $c$ is at least $\sqrt{2}/6 \doteq 0.2357$, so one subsegment is slightly less than a quarter as long as the original segment.

**Theorem 13.** *Suppose that any two incident segments are separated by an angle of at least* $60°$*, and a triangle is considered to be skinny if its circumradius-to-shortest edge ratio is larger than* $B \geqslant 1$*. Ruppert's algorithm with range-restricted segment splitting will terminate, with no triangulation edge shorter than* $\text{lfs}_{\min}/6$.

**Proof.** Omitted. □

Chew's algorithm makes it possible to use narrower illegal ranges. If the input PSLG has no acute angles, a subsegment midpoint with parent $p$ cannot have an insertion radius smaller than $r_p \cos\theta$ (Lemma 5), so the geometric width of each illegal range only needs to be $1/\cos\theta$. For instance, if one uses Chew's algorithm with $\theta = 30°$, or Ruppert's algorithm with diametral lenses, one may use illegal ranges having a geometric width of $2/\sqrt{3} \doteq 1.15$ instead of $\sqrt{2} \doteq 1.41$. In this case, legal segment lengths are of the form $c2^x$, where $c \in [1, \sqrt{3})$, and $x$ is an integer.

Because the legal range is wider, and the illegal range narrower, splitting an illegal segment to yield legal subsegments is easier. Chew handles illegal segments by trisecting them. One can do better by splitting them into two pieces, just unevenly enough to ensure that both subsegment lengths are legal. The following recipe is suggested.

- If $c \in [\sqrt{3}, 1 + \frac{\sqrt{3}}{3})$, then $c_1 = 1$ and $c_2 = c - c_1$.
- If $c \in [1 + \frac{\sqrt{3}}{2}, 2)$, then $c_1 = \frac{\sqrt{3}}{2} - \varepsilon$ and $c_2 = c - c_1$.

The most unbalanced split occurs if $c$ is $\sqrt{3}$. In this case, the ratio between $c_2$ and $c$ is approximately $1 - 1/\sqrt{3} \doteq 0.4226$, which isn't much worse than bisection.

For comparison, consider how Chew [10] guarantees that his algorithm terminates for an angle bound of 30°. Chew employs range-restricted segment splitting, but uses only one illegal range instead of an infinite sequence of ranges. For an appropriate value $h$ (see Chew for details, but one could use $h = \mathrm{lfs}_{\min}/2$), Chew declares the range $(\sqrt{3}h, 2h)$ illegal; subsegments with lengths between $2\sqrt{3}h$ and $4h$ are trisected rather than bisected. Hence, no edge shorter than $h$ ever appears.

There are two disadvantages of using a single illegal range, rather than an infinite series of illegal ranges. The first is the inconvenience of computing $h$ in advance. The second and more fundamental problem is that if small angles are present in the input PSLG, edges shorter than $h$ may arise anyway. The Terminator and range-restricted subsegment splitting mix well, but the Terminator requires an infinite series of illegal ranges.

How may the Terminator use range-restricted subsegment splitting? Modified segment splitting using concentric circular shells has priority over range-restricted subsegment splitting. Cluster subsegments are split to power-of-two lengths, and are thus legal. If a subsegment is not part of a subsegment cluster, it is split using the rules of range-restricted subsegment splitting. Hence, every segment may undergo up to three unbalanced splits: one for each end of the segment (using concentric shells), and one more if the middle subsegment has an illegal length. The only modification that must be made to Theorem 11 to prove that the Terminator still terminates is to account for the third unbalanced split (which can only happen a finite number of times). The Terminator's bound on the smallest angle (Theorem 12) still applies, with no change to the proof. Angles not near small input angles are guaranteed to be between 30° and 120°.

It does not appear to be possible to prove that Delaunay refinement with range-restricted segment splitting produces nicely graded or size-optimal meshes with circumradius-to-shortest edge ratios that are very close to one. The theoretical difficulty is that if a mesh contains a long segment with a small local feature size at one end, the small feature size could (in principle) propagate along the whole length of the segment. A short subsegment at one end of the segment might indirectly cause its neighboring subsegment to be split until the neighbor is the same length. The neighboring subsegment might then cause its neighbor to be split, and so on down the length of the segment.

As Fig. 37 demonstrates, however, even if Ruppert's algorithm with diametral circles is used, a chain reaction severe enough to compromise the grading of the mesh only seems to occur in practice if the quality bound is less than about 0.92 (corresponding to an angle of about 33°)!

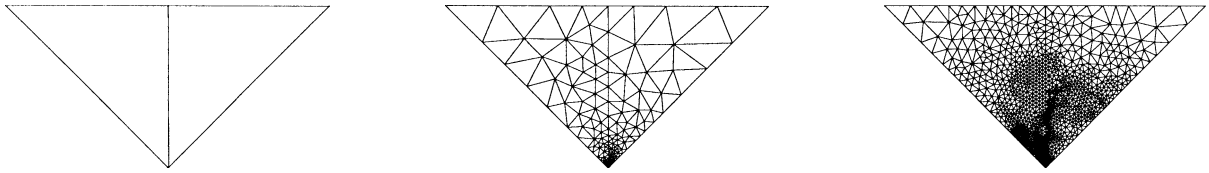

(a) (b) (c)

Fig. 37. (a) A PSLG with a tiny segment at the bottom tip. (b) With a minimum angle of 32° ($B \doteq 0.944$), Ruppert's algorithm creates a well-graded mesh, despite the lack of theoretical guarantees. (c) With a minimum angle of 33.5° ($B \doteq 0.906$), grading is poor.

The meshes in this figure were generated without range-restricted segment splitting, which is useful as a theoretical construct but unnecessary in practice. There is a good deal of "slack" in the inequalities that underlie the proofs of termination, because not every vertex has the smallest possible insertion radius relative to its parent. As a result of this slack, any Delaunay refinement algorithm that handles boundaries in a reasonable way seems to achieve angle bounds higher than 30°.

## 8. Conclusions

The intuition governing Delaunay refinement arises from an understanding of the relationship between the insertion radii of parents and their children. Hence, I use flow graphs to demonstrate these relationships. This analysis technique brings clarity to ideas that otherwise might be hidden within proofs. For instance, Fig. 13 provides an immediate explanation for why Ruppert's algorithm achieves an angle bound of up to 20.7° (which corresponds to a circumradius-to-shortest edge ratio of $\sqrt{2}$). The same analysis can be found in Ruppert's paper, but the underlying intuition is obscured by the mathematics.

The flow graphs pointed my way to a variety of improvements to Delaunay refinement and its analysis.

- The Terminator solves the problem of small input angles by preventing mesh vertices from having descendants with smaller insertion radii.
- A new analysis of Chew's algorithm arose from my efforts to understand the relationship between segment midpoints and their parents, a relationship reflected in the flow graph of Fig. 17.
- The flow graphs sparked my recognition of the fact that a better quality bound can be applied in the interior of the mesh, as illustrated in Fig. 35.
- Range-restricted segment splitting is a generalization of Chew's method for weakening the spiral of diminishing insertion radii.

Simple as the flow graphs are, they provided the clues that helped to unearth most of the new results in this article. Even more interestingly, they illuminate the way to extending most of the ideas discussed in this article to three-dimensional mesh generation [30,31]. Table 1 summarizes the angle bounds of the two-dimensional Delaunay refinement algorithms.

The problem of meshing PSLGs with tiny angles is harder than most researchers recognized. The negative result on quality triangulations in Section 5 comes as a surprise; many of us have been laboring under the false assumption that arbitrary PSLGs could be triangulated without creating new small angles. The recognition that this feat is impossible helps point the way to strategies for minimizing

Table 1
Angle bounds for the Delaunay refinement algorithms described in this article. The bounds in the first two rows apply only sufficiently far from small input angles. $\phi$ is the smallest input angle. The 30° bounds in the second row depend on the use of range-restricted segment splitting

| | Proven bounds on the minimum angle | | |
|---|---|---|---|
| | Diametral circles | Diametral lenses | Chew's algorithm |
| Graded | 20.70° | 25.65° | 26.56° |
| Uniform | 30° | 30° | 30° |
| Terminator | $\arcsin[\sin(\phi/2)/\sqrt{2}]$ | $\arcsin[(\sqrt{3}/2)\sin(\phi/2)]$ | n/a |

the unavoidable damage that small input angles can cause. The method suggested in Sections 6.3 and 6.4 is rather elaborate, but rewards the effort with good triangulations.

## Appendix A. Implementing Delaunay refinement

Pseudocode for the Terminator is provided in Figs. A.1 and A.2. This pseudocode implements both the Terminator with diametral circles from Section 6.3, and the Terminator with diametral lenses from Section 6.4.

After the initial triangulation is constructed, Line 2 removes all exterior triangles (those not in the triangulation domain) before Delaunay refinement begins. By contrast, in Ruppert's presentation [27], Delaunay refinement proceeds first. One of the reasons for removing exterior triangles first is discussed in Section 7.1: so that small exterior features do not bring forth unnecessarily small triangles. Fig. A.3 illustrates another reason. If the entire convex hull of the triangulation domain is triangulated, the boundary edges of the convex hull must be treated as segments, and spurious small angles and features may form. If an input vertex lies just inside the convex hull, then the local feature size near the vertex may be artificially reduced to an arbitrarily small distance. An arbitrarily small angle may also appear with dastardly stealth, as the figure shows. If the Terminator is not used, the user might be mystified why Ruppert's or Chew's algorithm fails to terminate on what appears to be an easy PSLG. In fact, it was this example that first made the negative result of Section 5 evident to me.

Early removal of extraneous triangles solves this problem, as Fig. A.3(d) shows. It also ensures that if two segments are separated by a small angle within a hole or concavity, where the region between the segments is not part of the triangulation domain, the small angle will have no effect on meshing.

During Delaunay refinement, the pseudocode maintains a queue $Q_t$ of skinny and oversized triangles and a queue $Q_s$ of encroached subsegments. (Chew's algorithm does not require the latter queue, as only one subsegment may be encroached at a time.) After the initial constrained Delaunay triangulation is constructed, the queue $Q_s$ is initialized by testing each segment of the initial triangulation for encroachment. After all the encroached segments are split, the queue $Q_t$ is initialized by testing the size and angles of each triangle in the triangulation. Both queues are maintained throughout Delaunay refinement. $Q_s$ rarely contains more than a few items, except at the beginning of Delaunay refinement (Lines 3–6), when it may contain many.

```
DELAUNAYTERMINATOR(X, θ, δ)
{ X is a segment-bounded PSLG. θ is the minimum allowable angle.}
{ δ(t) is a boolean function that returns true if triangle t }
{ is too large (as determined by the user), false otherwise.}
1   Construct T, the constrained Delaunay triangulation of X
2   Remove from T all triangles not in the triangulation domain
3   for each segment s ∈ X
4     if s is encroached
5       ENQUEUE(s, Q_s)    {Q_s is the queue of encroached subsegments}
6   SPLITENCROACHEDSUBSEGMENTS(0, false)
7   for each triangle t ∈ T
8     if δ(t) or t has a (non-input) angle less than θ
9       ENQUEUE(t, Q_t)    {Q_t is the queue of bad triangles}
10  while queue Q_t is not empty
11    t ← DEQUEUE(Q_t)
12    if t still exists in T
13      c ← the circumcenter of t
14      E ← the set of subsegments that c encroaches upon
15      if E = ∅
16        Insert c into T, maintaining constrained Delaunay property
17        NEWVERTEX(c, θ, δ)    {check subsegments and triangles}
18      else
19        d ← r_g, where g is youngest endpoint of shortest edge of t
                {alternatively, d ← length of shortest edge of t }
20        for each s ∈ E
21          if δ(t) or SPLITPERMITTED(s, d)
22            ENQUEUE(s, Q_s)
23        if queue Q_s is not empty
24          ENQUEUE(t, Q_t)    {Put t back for another try}
25          SPLITENCROACHEDSUBSEGMENTS(θ, δ)
26  return T
```

Fig. A.1. Code for the Terminator, the Delaunay refinement algorithm recommended in this article. The subroutines SPLITPERMITTED, SPLITENCROACHEDSUBSEGMENTS, and NEWVERTEX appear in Fig. A.2. Subsegment encroachment can be defined using either diametral circles or diametral lenses.

Each vertex insertion may add new members to either queue. After a new vertex $v$ is inserted, the subroutine NEWVERTEX identifies and enqueues all the bad triangles thus created, and all the subsegments encroached upon by $v$. If $v$ was inserted into a subsegment, the two subsegments resulting from the split must also be tested for encroachment (subroutine SPLITENCROACHEDSUBSEGMENTS, Lines 46–49).

Fortunately, testing a subsegment for encroachment (Lines 4, 46, 48, 52) is a quick local operation. The algorithm must inspect only the one or two vertices that form triangles in conjunction with the subsegment. To see why, consider Fig. A.4(a). In the illustration, both vertices ($v$ and $w$) opposite the subsegment $s$ lie outside the diametral circle of $s$. Because the mesh is constrained Delaunay, each triangle's circumcircle encloses no vertex visible from the triangle's interior, and therefore the diametral circle of $s$ encloses no vertex visible from the relative interior of $s$. In general, if $s$ is encroached, then

```
SplitPermitted(s, d)
27  if s belongs to no subsegment cluster, s belongs to
                two subsegment clusters, or the length of s
                is not a power of two (within some tolerance)
28    return true
29  S ← the subsegment cluster that includes s
30  if S contains a subsegment shorter than s (within some tolerance)
31    return true
32  r_min ← |s| sin(φ_min/2), where φ_min is the smallest angle
                separating two subsegments in S.
33  if r_min ⩾ d
34    return true    {No new edge will be shorter than shortest existing edge}
35  return false

SplitEncroachedSubsegments(θ, δ)
36  while queue Q_s is not empty
37    s ← Dequeue(Q_s)
38    if s is still an edge of T
39      Let v be a splitting vertex in s
                (chosen using concentric circular shells)
{Lines 40–43 needed only when using diametral lenses}
40      Delete from T all free vertices visible from v inside
                the diametral circle of s,
                maintaining constrained Delaunay property
41      for each triangle t created by Line 40
42        if δ(t) or t has a (non-input) angle less than θ
43          Enqueue(t, Q_t)
44      Insert v into T, splitting s into s_1 and s_2 and
                maintaining constrained Delaunay property
45      NewVertex(v, θ, δ)
46      if s_1 is encroached
47        Enqueue(s_1, Q_s)
48      if s_2 is encroached
49        Enqueue(s_2, Q_s)

NewVertex(v, θ, δ)
50  for each triangle t ∈ T that has v as a vertex
51    e ← the edge of t opposite v
52    if e is a subsegment and v encroaches upon e
53      Enqueue(e, Q_s)
54    else if δ(t) or t has a (non-input) angle less than θ
55      Enqueue(t, Q_t)
```

Fig. A.2. Subroutines for the Terminator.

either $v$ or $w$ must lie on or inside its diametral circle. As Fig. A.4(b) shows, the same argument is true if diametral lenses are used instead of diametral circles, because a diametral lens is defined by circular arcs passing through a segment's endpoints.

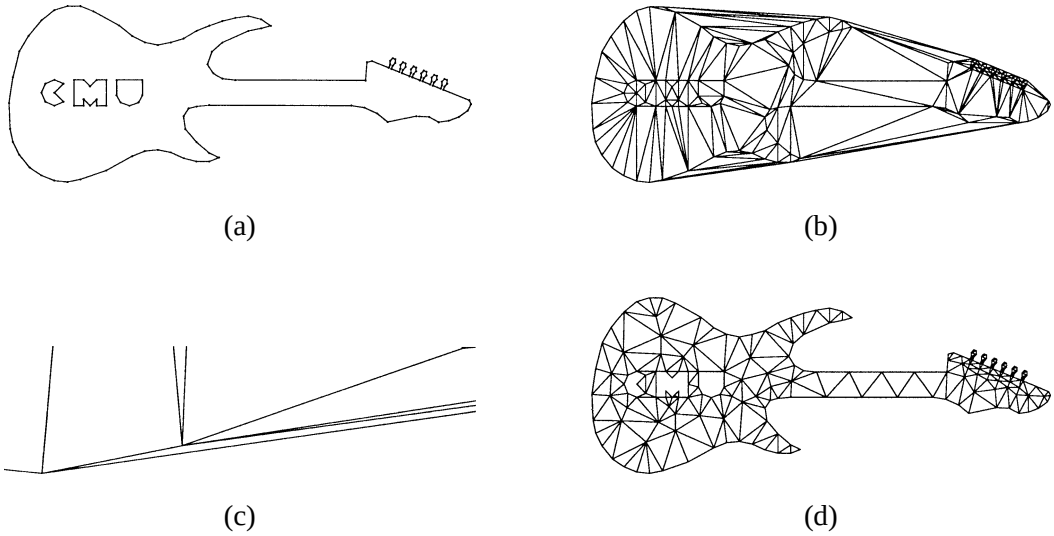


Fig. A.3. (a) Guitar PSLG. (b) Its constrained Delaunay triangulation. (c) Close-up of a small angle formed at the bottom of the guitar between a PSLG segment and a convex hull edge. (d) Mesh with 20° minimum angle. Exterior triangles were removed before applying Delaunay refinement.

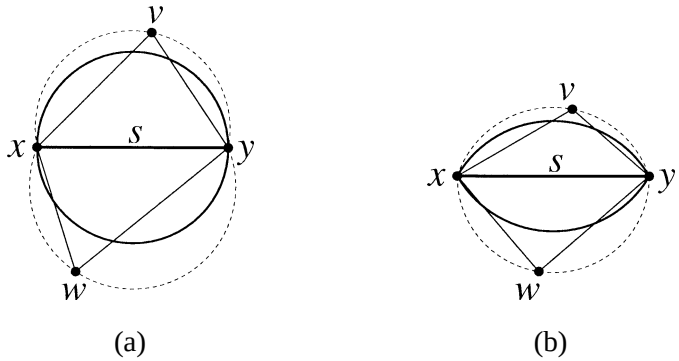


Fig. A.4. (a) If the apices (here, $v$ and $w$) of the triangles that contain a subsegment $s$ are outside the diametral circle of $s$, then no visible vertex lies in the diametral circle of $s$, because the triangles are constrained Delaunay. (b) The same statement is true for the diametral lens of $s$.

The test for encroached diametral circles is quite simple. Let $t$ be a triangle formed by a subsegment $s$ and a vertex $w$ opposite $s$. Let $x$ and $y$ be the endpoints of $s$. If the angle at $w$ is greater than or equal to 90°, then $w$ encroaches upon $s$; this condition is true if $(x - w) \cdot (y - w) \leqslant 0$. A diametral lens is encroached if the angle at $w$ is 120° or more, which is true if $(x - w) \cdot (y - w) \leqslant -|xw||yw|/2$.

Line 16 performs a Delaunay insertion of $c$, the circumcenter of a triangle $t$, into the triangulation. Before $c$ can be inserted, the triangle containing $c$ must be located. The potential difficulty is that general-purpose point location in a dynamically changing nonconvex triangulation is complicated. Fortunately, locating the circumcenter of a triangle is much easier and quicker than general point location. The circumcenter $c$ of $t$ is located by walking from the centroid of $t$ toward $c$. If the path is blocked by a

subsegment, then $c$ encroaches upon the subsegment, and the search may be abandoned. (The subsegment is encroached whether diametral circles or diametral lenses are used.) Because the mesh is segment-bounded, each search must either succeed or be foiled by an encroached subsegment.

To help in deciding whether to insert the circumcenter $c$, Line 14 finds the subsegments encroached upon by $c$. The simplest way to accomplish this is to insert $c$ into the triangulation, then check each edge that appears opposite $c$ in some triangle to see if it is a subsegment and if it is encroached upon by $c$ (just like the NEWVERTEX subroutine does, but without enqueueing the encroached subsegments). If $c$ does encroach upon one or more subsegments, $c$ must be deleted, restoring the mesh to its original form. The most efficient way to accomplish this is to record the sequence of edge flips performed by Lawson's algorithm when $c$ is inserted, then reverse the sequence if $c$ must be deleted. One caveat in using this approach: it is important that any "bad" triangles (too skinny or too large) that were in the queue $Q_t$ just before $c$ was inserted are still in the queue after $c$ is deleted.

If $c$ is rejected because it encroaches upon a subsegment, and at least one subsegment is split as a result, then $t$ is put back in the queue $Q_t$ (Line 24). Recall from the example of Fig. 7 that even if $c$ is rejected, it may be inserted later when Delaunay refinement attempts to split $t$ again. However, if the Terminator declines to split every segment $c$ encroaches upon, $t$ must *not* be put back in the queue, because an infinite loop might occur as the algorithm tries repeatedly to split $t$. For the same reason, it is also important that any triangles that were *not* in $Q_t$ just before $c$ was inserted are still *not* in $Q_t$ after $c$ is deleted, even if they are skinny.

Two different options are given for Line 19. These options are discussed briefly in Section 6.5. It takes more programming effort to determine $r_g$ than to determine the length of the shortest edge of $t$. The latter choice is slightly more conservative about splitting subsegment clusters, so it may produce a mesh with fewer triangles, but it may also leave more skinny triangles behind. I have not implemented the former choice, so this comparison is speculative.

Line 40 asks that a free vertex be deleted from the mesh while the constrained Delaunay property is preserved. The simple $O(m \log m)$-time vertex deletion algorithm of Devillers [14] is suitable (where $m$ is the degree of the vertex), but the typical vertex degree is usually so small in practice that even a simple $O(m^2)$-time algorithm will suffice, and perhaps run faster.

The number of triangles in the final mesh depends on the order in which skinny triangles are split, especially when a strong angle bound is used. Fig. A.5 demonstrates how sensitive Ruppert's algorithm is to the order. For this example with a 33° minimum angle, a heap of skinny triangles indexed by their smallest angle confers a 35% reduction in mesh cardinality over a first-in first-out (FIFO) queue. (This difference is typical for strong angle bounds, but thankfully seems to disappear for small angle bounds.) This improvement probably occurs because circumcenters of very skinny triangles are likely to eliminate more skinny triangles than circumcenters of mildly skinny triangles. Unfortunately, a heap is slow for large-cardinality meshes, especially when bounds on the maximum triangle size force all of the triangles into the heap. Delaunay refinement usually takes $O(n)$ time in practice, where $n$ is the number of vertices inserted, but the use of a heap increases the complexity to $O(n \log n)$.

A solution that seems to work well in practice is to use 64 FIFO queues, each representing a different interval of circumradius-to-shortest edge ratios. Oddly, it is counterproductive in practice to order good-quality triangles, so just one queue is used for good-quality but too-large triangles whose ratios are all roughly smaller than 0.8, corresponding to a minimum angle of about 39°. Triangles with larger quality ratios are partitioned among the remaining queues. When a skinny triangle is chosen for splitting, it is taken from the "worst" nonempty queue. An ordered queue of nonempty queues is maintained so that

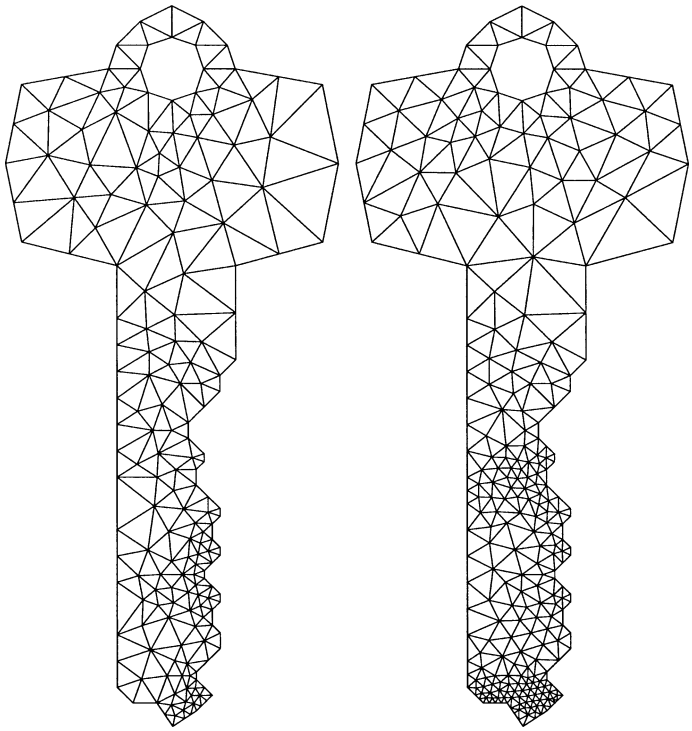

Fig. A.5. Two meshes with a 33° minimum angle. The left mesh, with 290 triangles, was formed by always splitting the worst existing triangle. The right mesh, with 450 triangles, was formed by using a first-come first-split queue of skinny triangles.

a skinny triangle may be chosen quickly. This method yields meshes comparable with those generated using a heap, but is only slightly slower than using a single queue.

## Acknowledgements

Thanks to Omar Ghattas, Thomas Gross, Gary Miller, David O'Hallaron, Jim Ruppert, James Stichnoth, Dafna Talmor, and Daniel Tunkelang for comments and conversations that greatly improved this document.

## References

[1] I. Babuška, A.K. Aziz, On the angle condition in the finite element method, SIAM J. Numer. Anal. 13 (2) (1976) 214–226.
[2] B.S. Baker, E. Grosse, C.S. Rafferty, Nonobtuse triangulation of polygons, Discrete Comput. Geom. 3 (2) (1988) 147–168.
[3] M. de Berg, M. van Kreveld, M. Overmars, O. Schwarzkopf, Computational Geometry: Algorithms and Applications, Springer-Verlag, Berlin, 1997.

[4] M. Bern, D. Eppstein, Mesh generation and optimal triangulation, in: D.-Z. Du, F. Hwang (Eds.), Computing in Euclidean Geometry, Lecture Notes Series on Computing, Vol. 1, World Scientific, Singapore, 1992, pp. 23–90.
[5] M. Bern, D. Eppstein, J.R. Gilbert, Provably good mesh generation, J. Comput. System Sci. 48 (3) (1994) 384–409.
[6] A. Bowyer, Computing Dirichlet tessellations, Computer J. 24 (2) (1981) 162–166.
[7] G.F. Carey, J.T. Oden, Finite Elements: Computational Aspects, Prentice-Hall, Englewood Cliffs, NJ, 1984.
[8] L.P. Chew, Constrained Delaunay triangulations, Algorithmica 4 (1) (1989) 97–108.
[9] L.P. Chew, Guaranteed-quality triangular meshes, Tech. Rept. TR-89-983, Department of Computer Science, Cornell University, Ithaca, NY, 1989.
[10] L.P. Chew, Guaranteed-quality mesh generation for curved surfaces, in: Proceedings of the Ninth Annual ACM Symposium on Computational Geometry, San Diego, CA, 1993, pp. 274–280.
[11] L.P. Chew, Guaranteed-quality Delaunay meshing in 3D, in: Proceedings of the Thirteenth Annual ACM Symposium on Computational Geometry, 1997, pp. 391–393.
[12] K.L. Clarkson, P.W. Shor, Applications of random sampling in computational geometry, II, Discrete Comput. Geom. 4 (1) (1989) 387–421.
[13] T.K. Dey, C.L. Bajaj, K. Sugihara, On good triangulations in three dimensions, Internat. J. Comput. Geom. Appl. 2 (1) (1992) 75–95.
[14] O. Devillers, On deletion in Delaunay triangulations, in: Proceedings of the Fifteenth Annual ACM Symposium on Computational Geometry, 1999, pp. 181–188.
[15] R.A. Dwyer, A faster divide-and-conquer algorithm for constructing Delaunay triangulations, Algorithmica 2 (2) (1987) 137–151.
[16] W.H. Frey, Selective refinement: A new strategy for automatic node placement in graded triangular meshes, Internat. J. Numer. Methods Engrg. 24 (11) (1987) 2183–2200.
[17] L.J. Guibas, J. Stolfi, Primitives for the manipulation of general subdivisions and the computation of Voronoi diagrams, ACM Trans. Graphics 4 (2) (1985) 74–123.
[18] M.T. Jones, P.E. Plassmann, Adaptive refinement of unstructured finite-element meshes, Finite Elements in Analysis and Design 25 (1997) 41–60.
[19] C.L. Lawson, Software for $C^1$ surface interpolation, in: J.R. Rice (Ed.), Mathematical Software III, Academic Press, New York, 1977, pp. 161–194.
[20] D.-T. Lee, A.K. Lin, Generalized Delaunay triangulations for planar graphs, Discrete Comput. Geom. 1 (1986) 201–217.
[21] D.-T. Lee, B.J. Schachter, Two algorithms for constructing a Delaunay triangulation, Internat. J. Comput. Inform. Sci. 9 (3) (1980) 219–242.
[22] G.L. Miller, D. Talmor, S.-H. Teng, Optimal good-aspect-ratio coarsening for unstructured meshes, in: Proceedings of the Eighth Annual ACM Symposium on Discrete Algorithms, New Orleans, LA, 1997, pp. 538–547.
[23] G.L. Miller, D. Talmor, S.-H. Teng, N. Walkington, A Delaunay based numerical method for three dimensions: Generation, formulation, and partition, in: Proceedings of the Twenty-Seventh Annual ACM Symposium on the Theory of Computing, Las Vegas, NV, 1995, pp. 683–692.
[24] S.A. Mitchell, Cardinality bounds for triangulations with bounded minimum angle, in: Proceedings of the Sixth Canadian Conference on Computational Geometry, Saskatoon, Saskatchewan, Canada, 1994, pp. 326–331.
[25] J. Ruppert, A new and simple algorithm for quality 2-dimensional mesh generation, Tech. Rept. UCB/CSD 92/694, University of California at Berkeley, Berkeley, CA, 1992.
[26] J. Ruppert, A new and simple algorithm for quality 2-dimensional mesh generation, in: Proceedings of the Fourth Annual ACM Symposium on Discrete Algorithms, 1993, pp. 83–92.

[27] J. Ruppert, A Delaunay refinement algorithm for quality 2-dimensional mesh generation, J. Algorithms 18 (3) (1995) 548–585.
[28] R. Seidel, Backwards analysis of randomized geometric algorithms, Tech. Rept. TR-92-014, International Computer Science Institute, University of California at Berkeley, Berkeley, CA, 1992.
[29] J.R. Shewchuk, Triangle: Engineering a 2D quality mesh generator and Delaunay triangulator, in: M.C. Lin, D. Manocha (Eds.), Applied Computational Geometry: Towards Geometric Engineering, First ACM Workshop on Applied Computational Geometry, Lecture Notes in Computer Science, Vol. 1148, Springer-Verlag, Berlin, 1996, pp. 203–222.
[30] J.R. Shewchuk, Tetrahedral mesh generation by Delaunay refinement, in: Proceedings of the Fourteenth Annual ACM Symposium on Computational Geometry, Minneapolis, MN, 1998, pp. 86–95.
[31] J.R. Shewchuk, Mesh generation for domains with small angles, in: Proceedings of the Sixteenth Annual ACM Symposium on Computational Geometry, Hong Kong, 2000, pp. 1–10.
[32] D.F. Watson, Computing the $n$-dimensional Delaunay tessellation with application to Voronoi polytopes, Computer J. 24 (2) (1981) 167–172.